Available online at www.sciencedirect.com
ScienceDirect
Journal of Volcanology and Geothermal Research 163 (2007) 1–33
Journal of volcanology and geothermal research
www.elsevier.com/locate/jvolgeores

Geology and hydrogeochemistry of the Jungapeo CO_2-rich thermal springs, State of Michoacán, Mexico

Claus Siebe [a,*], Fraser Goff [b], María Aurora Armienta [a], Dale Counce [c], Robert Poreda [d], Steve Chipera [c]

[a] *Departamento de Vulcanología, Instituto de Geofísica, Universidad Nacional Autónoma, de México, Coyoacán 04510, México D.F., México*
[b] *Department of Earth and Planetary Sciences, University of New Mexico, Albuquerque, NM 87131, USA*
[c] *Earth and Environmental Sciences Division, Los Alamos National Lab., Los Alamos, NM 87544, USA*
[d] *Department of Earth and Environmental Sciences, University of Rochester, Rochester, NY 14627, USA*

Received 19 April 2006; received in revised form 28 March 2007; accepted 30 March 2007
Available online 20 April 2007

Abstract

We present the first geothermal assessment of the Jungapeo CO_2-rich mineral springs, which are located in the eastern part of Michoacán State (central Mexico) at the southern limit of the Trans-Mexican Volcanic Belt. All but one of the >10 springs occur at the lower contact of the distal olivine-bearing basaltic andesite lavas of the Tuxpan shield, a 0.49- to 0.60-Ma-old cluster of monogenetic scoria cones and lava flows. The Tuxpan shield has a maximum radius of 6 km and was constructed on top of a folded and faulted Cretaceous basement consisting largely of marine limestones, marls, and shales. The mineral waters are characterized by moderate temperatures (28 to 32 °C), mild acidity (pH from 5.5 to 6.5), relatively high discharge rates, effervescence of CO_2 gas, clarity at emergence and abundant subsequent precipitation of hydrous iron, silica oxides, and carbonates around pool margins and issuing streamlets. Chemical and isotopic (deuterium, oxygen, and tritium) analyses of water and gas samples obtained during the period 1991–1997 indicate that the springs are largely composed of meteoric water from a local source with relatively short residence times (water ages of 7 to 25 years). Spring waters are chemically characterized by moderate SiO_2, Ca+Mg nearly equal to Na+K, high HCO_3, moderate to low Cl, low F and SO_4, high B, moderate Li, while Br and As are low. In contrast, Fe+Mn is exceptionally high. Thus, the Jungapeo waters cannot be regarded as high-temperature geothermal fluids. Instead, they resemble soda spring waters similar to other low-to-medium temperature soda waters in the world. Gas samples are extremely rich in CO_2 with no detectable geothermal H_2S or H_2 and very low contents of CH_4 and NH_3, indicating the gases are not derived from a high-temperature resource. Carbon-13 analyses of CO_2 show a narrow range (−6.7‰ and −7.2‰) that falls within the range for MORB CO_2. Thus, most CO_2 seems to originate from the mantle but some CO_2 could originate from thermal degradation of organic remains in underlying Cretaceous rocks. $^{3/4}$He ratios range from about 2 to 3 Rc/Ra, indicating that a small mantle/magmatic He component is present in the gases. In conclusion, the mineral waters are the surface expression of a low-temperature geothermal system of limited size that originates from the combined effects of a high regional heat flow and (possibly) the remnant heat released from subjacent basaltic andesite magma bodies that constitute the root zone of the Tuxpan shield.

Keywords: Jungapeo; geothermal assessment; Trans-Mexican Volcanic Belt; scoria cone; Tuxpan shield; geothermal waters; mineral springs; water and gas chemistry; stable and noble gas isotopes

* Corresponding author.
E-mail addresses: csiebe@geofisica.unam.mx (C. Siebe), candf@swcp.com (F. Goff).

0377-0273/$ - see front matter © 2007 Elsevier B.V. All rights reserved.
doi:10.1016/j.jvolgeores.2007.03.008

1. Introduction

The town of Jungapeo is located 15 km W of the small city of Zitácuaro in the eastern part of Michoacán State in central Mexico. This region of pleasant subtropical climate is at the southern limit of the Trans-Mexican Volcanic Belt (TMVB), an active subduction-related magmatic arc that crosses Mexico from the Pacific Ocean in the W to the Gulf of Mexico in the E (Fig. 1). The main river in the study area, the Río Tuxpan, flows in a N–S direction along a narrow gorge towards its confluence with the Río Balsas, some 120 km S of Jungapeo. At least ten CO_2-rich thermal springs occur along a narrow 6-km-long strip on the lower valley slope on the W margin of the Río Tuxpan (Figs. 1 and 2). Abundant pre-Hispanic pottery sherds found by us around the El Tular spring just outside Jungapeo, indicate that these springs did already attract people in remote times. While two of the springs (San José Purúa and Agua Blanca) were developed for tourism as spa-hotels in the 1950s (San José Purúa used to be a well-known first-class resort), all the other springs still remain poorly known and are only used by local peasants for recreational purposes. Despite their economic potential and location within a Quaternary volcano in the TMVB, a thorough discussion of the geologic and volcanic provenance of the springs, and detailed chemical and isotope analyses of the thermal fluids have never been published. The present study is intended to close this gap.

2. Geologic setting

Physiographically, the Jungapeo area is located at the trenchward front of the TMVB, right beyond the southern limit of the Mexican Altiplano, where the slopes rapidly descend into the depression occupied by the Balsas River. The regional basement includes Jurassic schists and Cretaceous limestones, marls, and shales, which crop out in valleys and narrow canyons (Petersen, 1989; McLeod, 1989). They are overlain by Oligocene volcanics of the Sierra Madre Occidental (Pasquaré et al., 1991) which in turn are capped by plateau-forming mafic lava flows. Younger Miocene to Quaternary volcanic rocks of the TMVB dominate the topography, mostly as silicic domes, scoria cones, and associated lavas (Blatter and Carmichael, 1998; Blatter et al., 2001).

West of the study area, the Tzitzio anticline (Mesozoic folded marine sediments) lacks a young volcanic cover and creates a "gap" or indentation in the volcanic front of the TMVB. The axis of the Tzitzio anticline is oriented in a NNW direction. Most of the lineaments observable on satellite images, aerial photographs, and topographic maps of the Jungapeo region are also oriented in this direction. Further west of this indentation or "gap" extends the main part of the Michoacán–Guanajuato Volcanic Field (Hasenaka and Carmichael, 1985, 1987), an area of ca. 40,000 km^2 that contains hundreds of scoria cones including the historic eruption (1943–1952) of Paricutin (Luhr and Simkin, 1993).

Northwest of the study area the Late Tertiary–Quaternary Los Azufres silicic complex (Dobson and Mahood, 1985; Pradal and Robin, 1994) hosts an extensive high-enthalpy geothermal system that has been developed in recent decades for the production of electricity by Mexico's national electric power company, the Comisión Federal de Electricidad. East of Zitácuaro a large group of silicic domes form the Zitácuaro Volcanic Complex (Capra et al., 1997). Most of these domes are mantled by an extensive plinian pumice fallout deposit that reaches >5 m in thickness in outcrops exposed along the new freeway near the town of La Dieta. Capra et al. (1997) dated this deposit by the conventional radiocarbon method at 31,350+1785/−1460 yr. BP (corrected for $\partial^{13}C$).

In this part of the TMVB, young volcanism has produced basaltic to andesitic scoria cones surrounded by lava shields, as well as silicic domes. Mafic to intermediate lavas typically display olivine, augite, and hypersthene phenocrysts with occasional hornblende ghosts. Plagioclase is frequently absent and quartz xenocrysts are common (Blatter and Carmichael, 1998). Pliocene volcanism in the Jungapeo area consists of olivine basalt lava flows which filled valleys between eroded mountains of older Tertiary ash flow deposits. The capping lava flow that forms Mesa del Campo (MC in Fig. 3) was dated by the $^{40}Ar/^{39}Ar$ method at 3.776±0.007 Ma (Blatter and Carmichael, 1998). Andesite lavas lower in the same sequence were dated by Petersen (1989) using the fission track method on zircons at 4.2±0.5 Ma and by the K–Ar method on hornblende at 6.0±0.7 Ma. The plateau-forming lava flows have been dissected since 3.8 Ma by the Río Tuxpan, which today runs in a narrow fault-controlled N–S oriented canyon. This erosional activity has lead to an inversion of the topography (due to the hardness of the capping rocks in former valleys that are now distinctive high mesas). These mesas are a characteristic feature of the landscape (Figs. 3 and 4). The vertical distance between the edge of the capping olivine basalt forming Mesa del Campo (1500 m asl) and the present river bed (1000 m asl) at a location at the western foot of

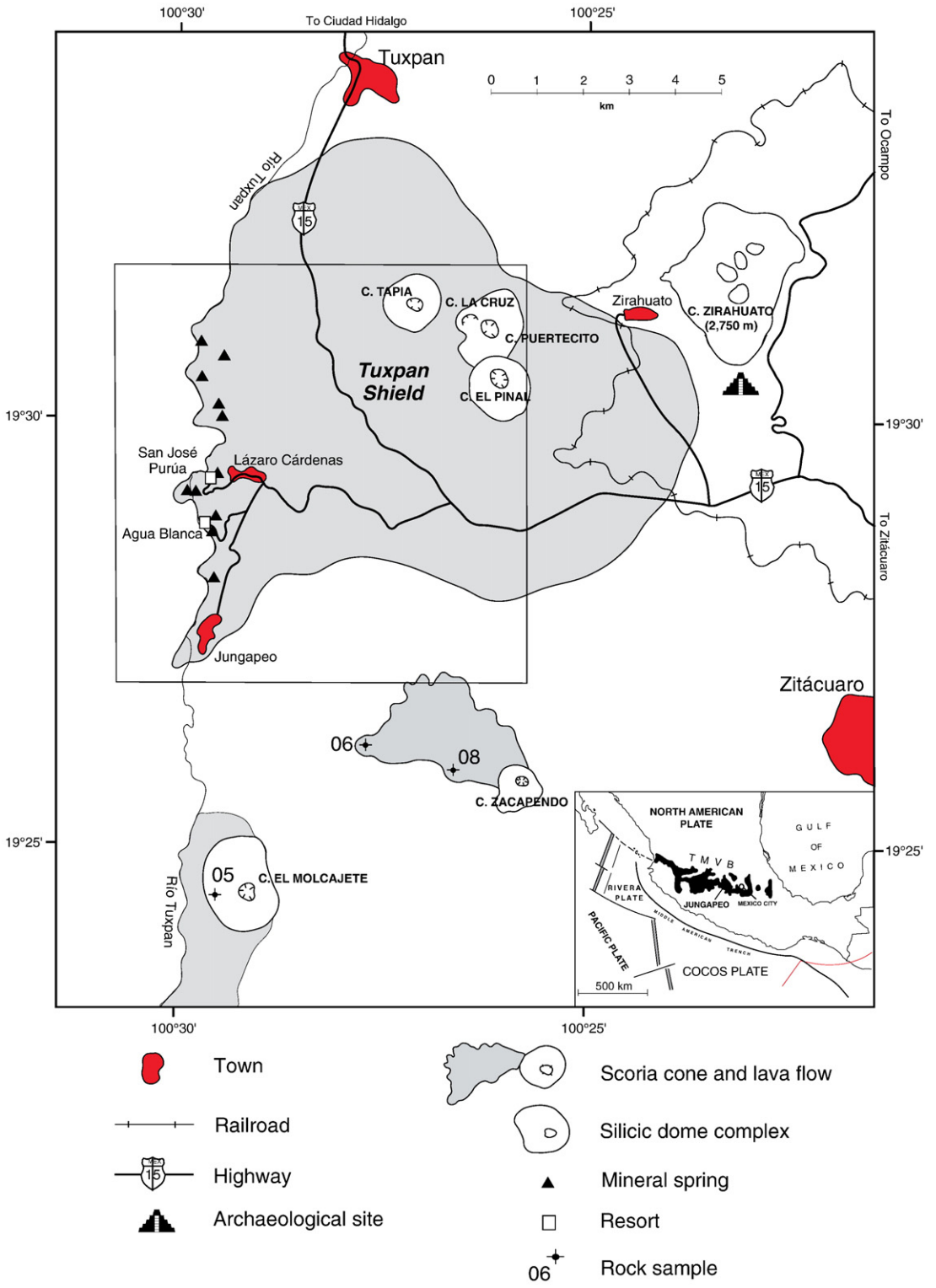

Fig. 1. Sketch map showing the location of the Jungapeo mineral springs (State of Michoacán) and their position within the central part of the Trans-Mexican Volcanic Belt (TMVB, see insert). Area outlined within quadrangle is shown in Fig. 2.

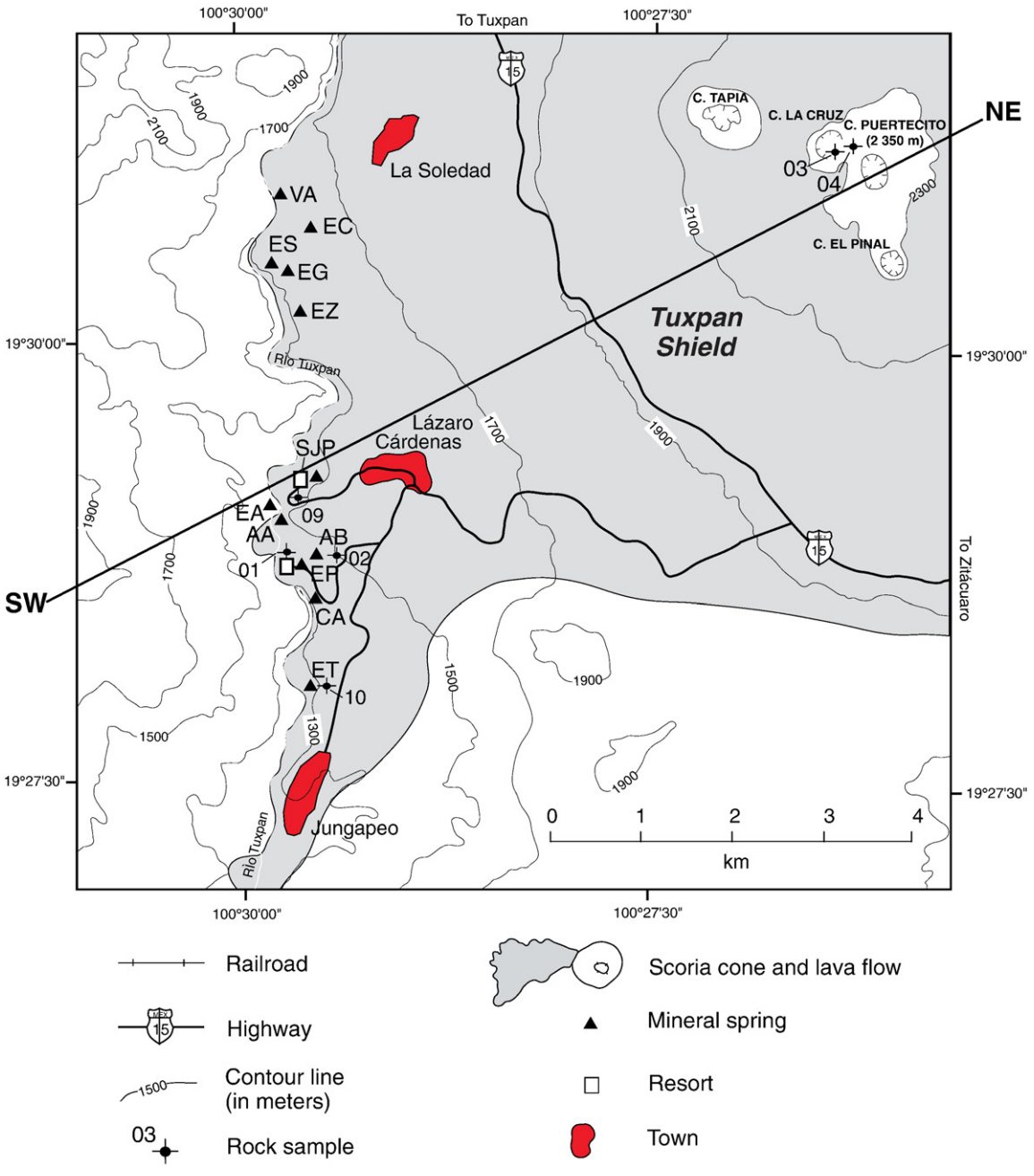

Fig. 2. Jungapeo area with spring sites on the east margin of the Río Tuxpan barranca. Most of the springs occur at the basal contact of the distal western lavas forming the shield crowned by the Cerro Tapia, Cerro La Cruz, Cerro Puertecito, and El Pinal scoria cones. VA = Varelas, ES = El Saúz, EG = El Guayabo, EZ = El Zapote, SJP = San José Purúa, EA = El Aguacate, AA = Agua Amarilla, AB = Agua Blanca, EP = El Puente, CA = Cañada Azul, ET = El Tular, EC = El Concreto.

El Molcajete scoria cone (Figs. 1, 3, and 4) is 500 m, implying an average down-cutting rate of 13.3 cm/ka.

Pleistocene volcanism is largely represented by scoria cones and associated lava flows. El Molcajete basaltic scoria cone is located 5.5 km to the south of Jungapeo on the W margin of the Río Tuxpan (Figs. 1, 3, and 4A). It has a characteristic conical shape with a well-preserved summit crater and an altitude of 400 m above surrounding ground. Its regular slopes are cut by several meters deep gullies and it erupted a 3.5-km-long lava flow that was emplaced along the former Tuxpan riverbed. Since then, the river has cut a new 100-m-

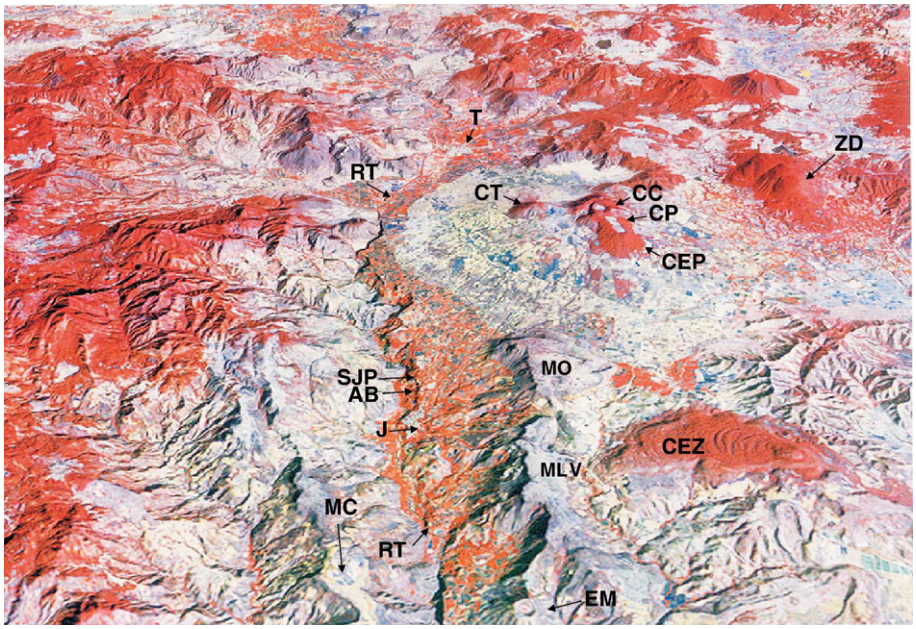

Fig. 3. Landsat Thematic Mapper satellite image (perspective view) showing the study area from the S toward the N. Most of the springs occur along the east margin of the Río Tuxpan (RT) at the basal contact of the lavas forming the shield surrounding the Cerro Tapia (CT), Cerro La Cruz (CC), Cerro El Puertecito (CP), and Cerro El Pinal (CEP) scoria cones. Other features mentioned in the text include ZD = Ziráhuato domes, CEZ = Cerro El Zacapendo andesite lava flow, J = Jungapeo, EM = El Molcajete scoria cone, T = Tuxpan, MO = Mesa de Ocurio, MLV = Mesa La Virgen, MC = Mesa del Campo.

deep channel along the W margin of the lava flow. Assuming the previously mentioned average down-cutting rate of 13.3 cm/ka, an approximate age of 0.752 Ma can be estimated. Such an old age is in contradiction with its youthful morphology and must therefore be considered with caution.

Cerro Las Hoyas (2470 m asl), Cerro La Cruz, and Cerro El Pinal (Figs. 1, 2, 3, and 4B, C) form a NNW-oriented alignment of amalgamated scoria cones that erupted along a normal fault. Cerro La Cruz has been quarried in recent years exposing 60- to 100-cm-thick feeder dikes that display the same NNW direction (Fig. 5). These scoria cones crown an asymmetric shield of basaltic andesite lavas. To the north the lava flows only reached 3 km from their source because the pre-existing Cerro La Campana dome impeded their flowage. The shield is widest towards the W and S, where the lava flows surrounded the Cerro Tapia (Fig. 3) and reached as far as 6 km from the source and plunged into the ancestral Río Tuxpan, where they formed a temporary dam. The river has since cut down 50 m into the bedrock along the margin of the shield (Fig. 3). Assuming an average down-cutting rate of 13.3 cm/ka, an age of 0.376 Ma was estimated for the shield. Surprisingly, this crude estimate coincides well with the $^{40}Ar/^{39}Ar$ ages ranging between 0.49 and 0.60 Ma obtained by Blatter et al. (2001) on groundmass separates of the basaltic andesite lavas. Because all but one of the springs considered in this study are located near the basal contact of lavas forming the Tuxpan shield, several lava samples were collected for analysis (see next section), in order to characterize this important aquifer.

To the E the shield lavas are overlain by the silicic Ziráhuato twin domes (Figs. 1 and 3). These domes are also aligned in a NNW direction and rise up to 650 m high above surrounding ground. The southern dome is slightly higher with an altitude of 2750 m asl. A rhyodacite sample from these domes was originally dated by Demant et al. (1975) and later corrected by Blatter and Carmichael (1998) at 51,000 ± 30,000 yr. BP. The southern dome collapsed during growth to the south as evidenced by a small landslide deposit that underlies pre-Hispanic archaeological ruins near the town of San Felipe Los Alzati.

The youngest volcanic feature in the area is the Zacapendo andesite lava flow (Figs. 1 and 3), which issued from a small breached cone and flowed 4 km to the WNW on an inclined plane until it ponded against the older Mesa La Virgen. The cone appears to be located on the SSE continuation of the NNW-oriented fault defined by the alignment of the cones crowning the

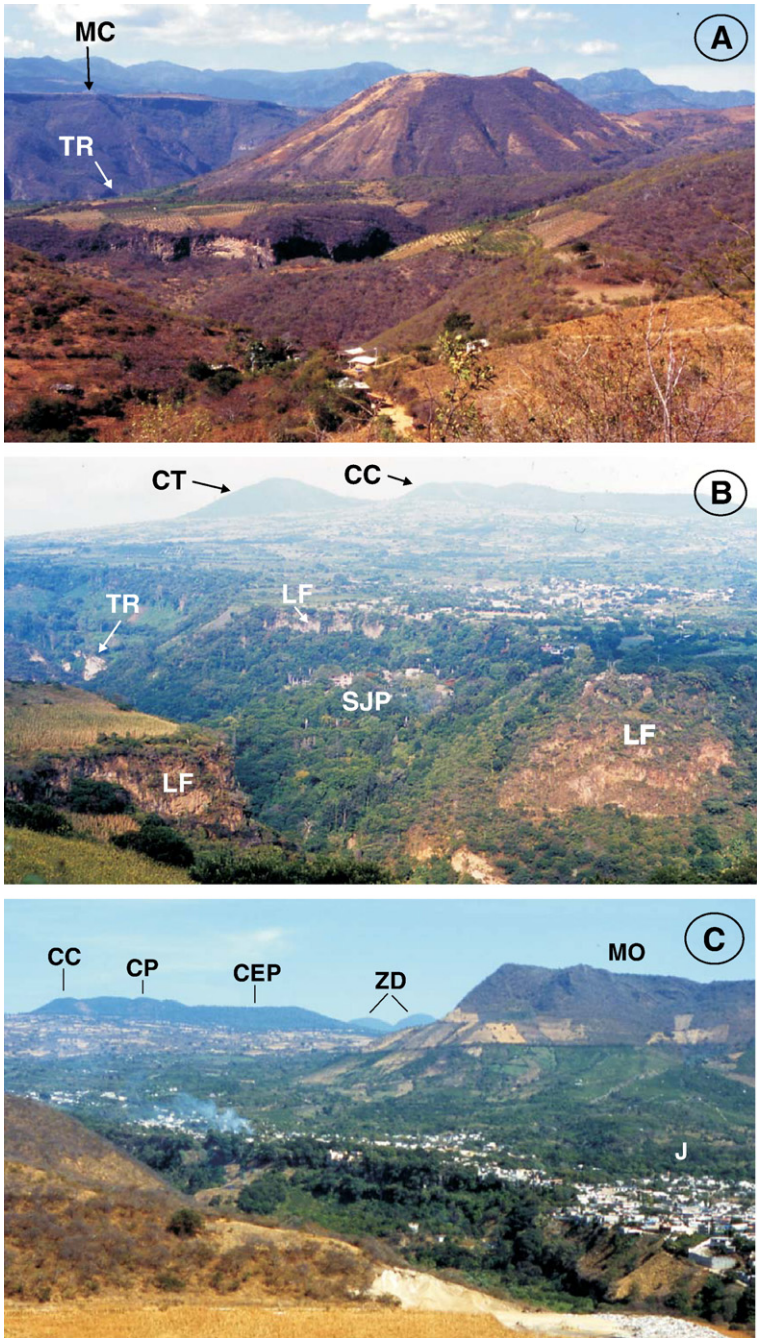

Fig. 4. (A) Molcajete basaltic scoria cone from the E. TR = Tuxpan River canyon, MC = Mesa del Campo. Photo taken April 1991. (B) View of the Tuxpan shield from Las Anonas (SW). LF = cliff-forming lava flows, TR = Tuxpan river, SJP = San José Purúa resort, CT = Cerro Tapia scoria cone, CC = Cerro La Cruz scoria cone. Photo taken October 29, 2005. (C) View of the Tuxpan shield from the road to Carrizal (from the SSW). In the foreground is the town of Jungapeo (J), which is built on a lava flow from the Tuxpan shield crowned by the NNW–SSE aligned scoria cones Cerro La Cruz (CC), Cerro El Puertecito (CP), and Cerro Pinal (CEP). The Ziráhuato dacite domes (ZD) and Mesa de Ocurio (MO) are also shown. Photo taken January 4, 2006. All photos by Claus Siebe.

Tuxpan shield. This lava flow, as well as older underlying plagioclase-free andesite lava flows was the focus of a recent petrologic study by Blatter and Carmichael (1998). According to $^{40}Ar/^{39}Ar$ dates provided by them, an older flow underneath Zacapendo is 0.371 ± 0.035 Ma, while a bomb from the culminating

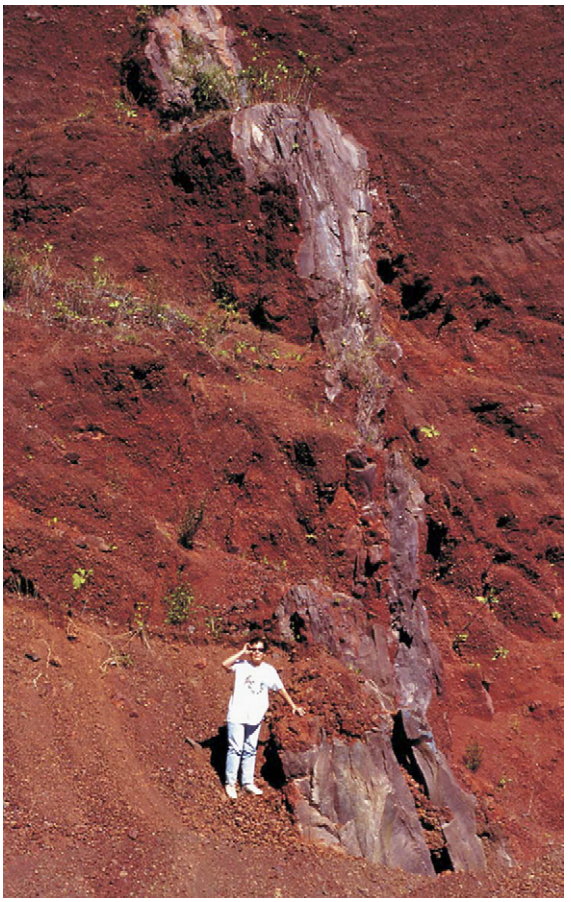

Fig. 5. One of the several feeder dikes of Cerro La Cruz cone (sampling locality 04 in Fig. 2) exposed at scoria quarry.

scoria cone that produced the Zacapendo lava flow is 0.236±0.139 Ma. Because of the poor soil cover of this flow and its well-preserved original surface features (marked flow fronts, distinct lateral margins, pressure ridges, etc., see also Fig. 3), we consider that this flow might be much younger (maybe only a few tens of thousands of years BP) than the reported age of 0.236± 0.139 Ma.

3. Methods

Thin sections of selected rock samples from the Tuxpan shield and other young volcanoes (Zacapendo and Molcajete) were examined by petrographic microscope at Instituto de Geofísica, Universidad Nacional Autónoma de México (UNAM). These samples were also analyzed by Inductively Coupled Plasma Emission Spectrometry (ICPES) and Instrumental Neutron Activation Analysis (INAA) for major and trace elements at Activation Laboratories Ltd., Ancaster, Canada. XRF analysis of a spring precipitate from Agua Blanca was obtained by J. Obenholzner (Vienna, Austria). Semi-quantitative X-ray diffraction analyses of Cretaceous calcareous shale fragments and Quaternary precipitates from inactive springs were determined at Los Alamos National Laboratory (LANL) using procedures described in Chipera and Bish (2002).

At the spring sites, temperatures were measured with either thermometers or thermocouple probes, pH was measured with a calibrated pH meter (UNAM samples) or with pH sensitive papers (LANL samples), and flow rates were measured with a bucket or beaker and a stopwatch (Table 4). Water samples for stable isotope analysis were collected raw into 30-ml glass bottles with Polyseal caps. The isotopes were determined at Southern Methodist University (Texas), Institute for the Study of Earth and Man using standard procedures. Samples for tritium analysis were collected raw into 500-ml glass bottles with Polyseal caps and analyses obtained from the Tritium Laboratory, University of Miami (Florida) using the electrolytic enrichment method (Ostlund and Dorsey, 1977).

Water samples from each site were obtained by filtering spring water (0.45 μl) brimful into two, pre-rinsed 125-ml polypropylene bottles. A few milliliters of water were then decanted from one bottle after which 10 to 20 ml of high-purity concentrated HNO_3 were added to the bottle to bring the resulting pH to ≤2. Bottles were sealed with Polyseal caps. The acidified sample was later used for cation and trace element analyses whereas the unacidified sample was used for anion analyses. Analyses conducted at UNAM were obtained using procedures outlined in Armienta and De la Cruz-Reyna (1995) whereas those conducted at LANL were determined by procedures listed in Werner et al. (1997, Table 1).

Gas samples were collected using large polypropylene funnels and Teflon tubing into 300-ml Pyrex flasks having double-port Teflon valves, which were filled with approximately 100 ml of carbonate-free 4 N NaOH (Fahlquist and Janik, 1992; Goff and Janik, 2002). Analyses were conducted at LANL using methods described by Werner et al. (1997) and by Goff and Janik (2002). Aliquots of headspace gases were transferred into 10-ml quartz vials using the LANL gas extraction system and sealed with a hydrogen torch. The contents of the vials were then analyzed for noble gases at the University of Rochester (New York) by procedures described in Poreda and Craig (1989). Aliquots of NaOH solutions were removed from the gas flasks into 50-ml glass bottles having Polyseal caps. Carbon-13 analyses of the dissolved CO_2 in these aliquots were

obtained from Geochron Laboratories (Massachusetts) by standard methods.

4. Mineralogical and chemical composition of volcanic and sedimentary rocks

Petrographic aspects of the volcanic and sedimentary rocks from the Jungapeo area were briefly described by McLeod (1989) and Petersen (1989). The young Zacapendo scoria cone and older underlying lavas are the only volcanic rocks in the area that have been studied in detail with modern analytical tools. Blatter and Carmichael (1998) provide chemical analyses of the Zacapendo lava flows (SiO_2 = 57.5–59.5 wt.%; MgO = 6.0–7.3 wt.%) whose phenocryst assemblage includes olivine, augite, bronzite, and xenocrystic quartz in a glassy groundmass of labradorite microlites and Ti-magnetite grains. In addition, these scientists carried out phase equilibria experiments and concluded that the magma equilibrated at 1050 °C and pressures around 1.2 kbar at H_2O-saturated conditions. This means that equilibration conditions for these hot wet plagioclase-free magmas could have been very shallow (~3 km).

In the present study we focused on the lavas of the Tuxpan shield because all but one (El Aguacate) of the mineral springs occur at the basal contact of these lavas. The spatial distribution of the springs indicates that these lavas serve as shallow aquifers and hence, a close genetic relationship between them. Samples 9703 and 9704 (dike and scoria) were collected near the vent at the Santa Cruz scoria cone. Additional four samples (9701, 9702, 9709, and 9710) were collected at the distal margins of the lava flows near the occurrence of the mineral springs. Samples from nearby young volcanoes Zacapendo (9706 and 9708) and Molcajete (9705) were analyzed for comparison. The location of sample sites is given in Figs. 1 and 2.

4.1. Petrography

Modal mineralogical analyses of selected samples are presented in Table 1. All the volcanic rocks studied are basaltic in appearance, ranging from dark to medium grey and dense to vesicular (up to 8.3 vol.%). In thin section, rocks from the Tuxpan shield display combinations of olivine and clinopyroxene phenocrysts in a groundmass of plagioclase and pyroxene microlites, glass, and opaques. Samples from the Santa Cruz cone (dike and scoria) differ notably in their texture but little in their mineralogical composition from samples collected from distal lava flows in the main spring area. The dike sample is more crystalline and has larger plagioclase crystals while the scoria is characterized by ovoid to round vesicles and a very glassy matrix. Lava flows show typical flow-alignment of crystals and elongated vesicles. All of these features reflect differences in the cooling history of the various samples. In the context of the present study, the most striking feature observable in rock samples is the degree of alteration of the olivine and clinopyroxene phenocrysts (Fig. 6). Olivines in scoria samples from the Santa Cruz cone are well preserved and contain clearly discernible cubic

Table 1
Modal mineralogical analyses (>600 points counted) of representative volcanic rocks from the Jungapeo area

Sample #	9701	9702	9704	9703	9705	9706	9708
Locality	Agua Blanca I	Agua Blanca II	C. La Cruz	C. La Cruz	Molcajete	Zacapendo	Zacapendo
	TS-lava	TS-lava	TS-dike	TS-scoria	Scoria	Lava	Lava
Rock type	BA	BA	BA	BA	BA	A	A
Lat.	19°28′46.5″	19°28′24.6″	19°31′05.5″	19°31′05.5″	19°24′15.7″	19°26′09.9″	19°25′28.1″
Long.	100°29′42.4″	100°29′22.5″	100°26′29.6″	100°26′29.6″	100°29′39.3″	100°27′58.2″	100°26′55.9″
Altitude	1393 m	1473 m	2330 m	2330 m	1273 m	1701 m	1711 m
Q_z (%)	0	0	0	0	0	0	3.16
Ol pc (%)	4.41	3.41	5.04	1.64	4.63	0	0
Opx pc (%)	0	0	0	0	0	2.26	3.32
Cpx pc (%)	0.65	0.33	1.95	0.18	2.57	6.13	3.66
Plag pc (%)	0	0	3.41	0	0	0	0
Plag mp (%)	37.09	56.91	21.14	13.64	8.23	0	0
Pyrox. mp (%)	2.61	17.89	23.09	1.82	0	10.65	9.30
Ol mp (%)	0	0	0.33	1.09	0	0.16	0
Opaque (%)	1.96	2.93	1.63	0	0.69	0.97	0.83
Groundmass (%)	53.28	18.53	43.41	81.63	83.88	79.83	79.73
Total (%)	**100.00**	**100.00**	**100.00**	**100.00**	**100.00**	**100.00**	**100.00**
Vesicles (%)	0	0.49	0	8.33	5.05	0	6.67

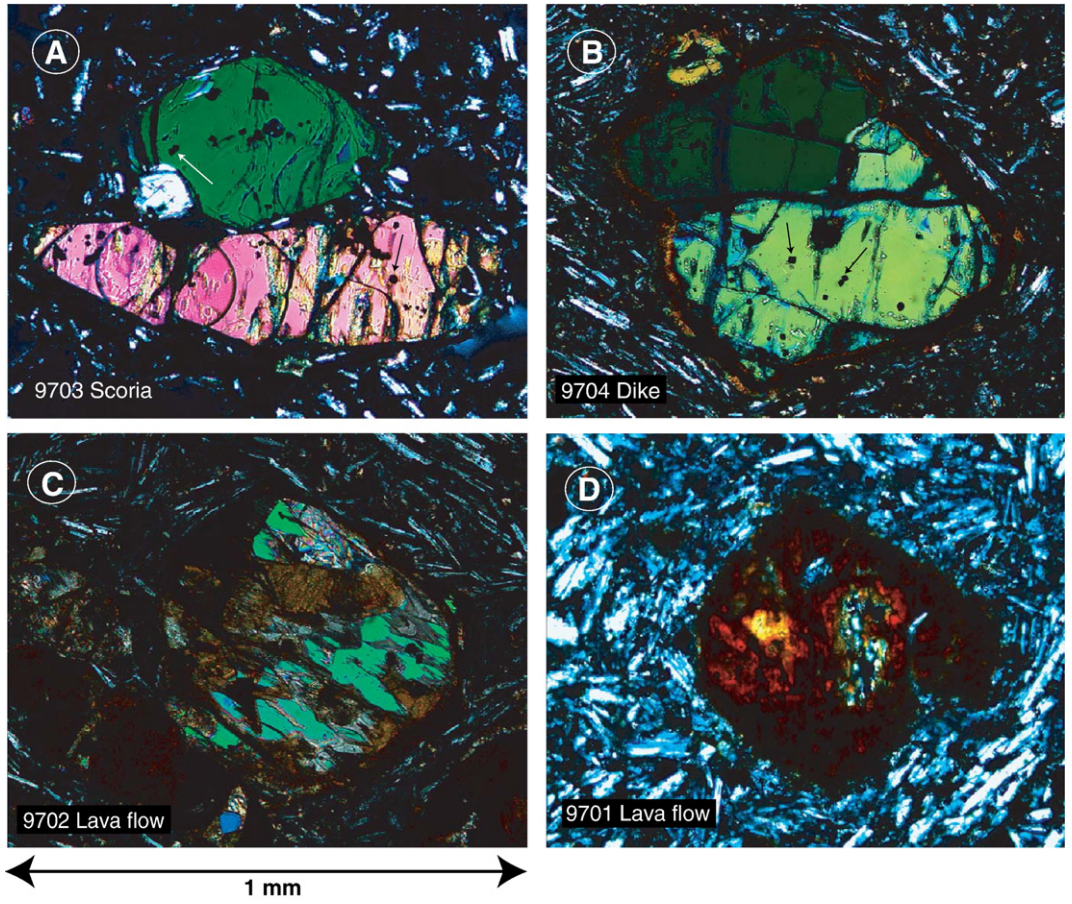

Fig. 6. Microphotographs (10×) of olivines in lava samples taken from the Tuxpan shield at increasing distance from the vent. (A) Unaltered olivines in scoria from the upper layers of Cerro La Cruz cone (locality 03 in Fig. 2). (B) Olivine with thin iddingsite rim in sample from dike (see also Fig. 5) feeding Cerro La Cruz cone (locality 04 in Fig. 2). Small cubic Cr-spinel crystals (see arrows) in the olivines are also observable. (C) Olivine largely transformed into iddingsite in lava flow at locality 02 (Fig. 2) at ca. 6 km from the vent. (D) Olivine completely altered into iddingsite at locality 01 near the Agua Blanca spring (Fig. 2). Note that the core of the olivine has been replaced with carbonates.

inclusions of Cr-spinel (Fig. 6A). Olivines in a dike feeding the cone display a thin rim of light-brown iddingsite (Fig. 6B). Samples from distal flows in the main spring area display olivines that are partly (Fig. 6C) to totally (Fig. 6D) replaced by iddingsite (Baker and Haggerty, 1967) and other alteration products. In the latter case cores of olivines tend to be hollow or filled with silica and carbonates. In such cases, vesicles in the lava flows are also filled by carbonates and silica while the glassy groundmass of the rock appears relatively fresh and intact (Fig. 6C and D). The above features indicate that the lavas forming the distal margin of the Tuxpan shield have been affected by low-temperature groundwater flow after their emplacement. The least stable minerals at near-atmospheric pressures and temperatures (olivine and clinopyroxene) have been transformed into iddingsite or even partly leached out and replaced by carbonates and silica at locations saturated with mineralized fluids. Samples obtained from the undersaturated non-vadose zone at high altitudes near the vent (e.g. Santa Cruz cone) are practically unaffected. This

Table 2
X-ray diffraction analyses of Cretaceous shale and Quaternary spring precipitates from Jungapeo area, Mexico (values in %)

Mineral	Shale	Precipitate #1 (white)	Precipitate #2 (gray)	Precipitate #3 (orange)
Quartz	7.1	0.1		
K-feldspar	2.2			
Plagioclase	12.8			
Mica	3.0			
Calcite	32.7	11.0		
Smectite	33.9			
Clinoptilolite	8.3			
Amorphous silica		85.9	100	85
Sepiolite?		3.0		
Goethite				15
Total	100	100	100	100

Table 3
Whole rock major and trace element analyses of the Tuxpan shield, Molcajete scoria cone, Zacapendo lava flow, and Agua Blanca water precipitate

	Analytical method	Detection limits	**9701**	9709	9710	9702	9704	9703	9705	9706	9708	
			TS-lava	TS-lava	TS-lava	TS-lava	TS-dike	TS-scoria	Scoria	Lava	Lava	Precipitate
Sample #			**Agua Blanca I**	S. Jose Purúa	El Tular	Agua Blanca II	C. La Cruz	C. La Cruz	Molcajete	Zacapendo	Zacapendo	Agua Blanca
Lat.			19°28′46.5″	19°29′04.9″	19°28′14.6″	19°28′24.6″	19°31′05.5″	19°31′05.5″	19°24′15.7″	19°26′09.9″	19°25′28.1″	19°28′41.8″
Long.			100°29′42.4″	100°29′38.3″	100°29′28.3″	100°29′22.5″	100°26′29.6″	100°26′29.6″	100°29′39.3″	100°27′58.2″	100°26′55.9″	100°29′40.1″
Altitude			1393 m asl	1475 m asl	1415 m asl	1473 m asl	2330 m asl	2330 m asl	1273 m asl	1701 m asl	1711 m asl	1330 m asl
(%)		**(%)**										
SiO_2	F-ICPES	0.01	53.12	53.87	53.92	54.10	54.49	54.58	55.04	59.34	59.55	13.95
TiO_2	F-ICPES	0.01	1.28	1.33	1.36	1.35	1.27	1.29	1.04	0.87	0.85	0.14
Al_2O_3	F-ICPES	0.01	16.03	16.75	16.95	16.46	16.61	16.58	16.65	14.83	14.63	0.74
Fe_2O_3t	F-ICPES	0.01	5.32	8.55	8.19	8.19	8.43	8.26	7.69	5.69	5.57	65.49
MnO	F-ICPES	0.01	0.31	0.13	0.12	0.37	0.12	0.12	0.13	0.09	0.09	0.05
MgO	F-ICPES	0.01	3.84	3.96	3.87	3.74	5.48	5.06	6.43	6.32	6.70	0.50
CaO	F-ICPES	0.01	7.78	7.44	6.90	8.35	7.26	7.12	7.04	7.45	7.33	4.21
Na_2O	F-ICPES	0.01	3.71	3.93	3.93	3.77	3.84	3.80	3.65	3.70	3.65	0.43
K_2O	F-ICPES	0.01	1.26	1.44	1.36	1.38	1.40	1.45	1.36	1.84	1.70	0.09
P_2O_5	F-ICPES	0.01	0.21	0.38	0.35	0.40	0.32	0.37	0.22	0.27	0.27	4.35
LOI			1.83	1.68	1.98	2.29	−0.22	0.45	−0.09	0.45	0.51	10.29
Total			**94.70**	**99.45**	**98.92**	**100.39**	**98.99**	**99.08**	**99.14**	**100.83**	**100.84**	**100.22**
(ppm)		**(ppm)**										
Be	F-ICPES	1	2	2	2	2	2	2	2	2	2	–
Sc	INAA	0.01	16.2	16.2	16.6	15.3	16.7	16.3	17.0	12.9	12.8	–
V	F-ICPES	1	130	148	154	146	139	142	135	111	108	–
Cr	INAA	0.5	119	112	145	93.3	101	93.8	178	204	237	–
Co	INAA	0.1	25.8	24.3	26.9	23.2	26.9	24.3	25.2	21.0	22.7	–

Ni	TD-ICPES	1	64	71	82	60	84	58	145	168	190	–
Cu	TD-ICPES	1	24	29	55	29	25	25	28	34	39	–
Zn	TD-ICPES	1	89	95	99	91	87	90	78	66	66	–
As	INAA	1	<1	<1	<1	<1	<1	<1	<1	<1	<1	–
Br	INAA	0.5	<0.5	0.6	<0.5	0.7	<0.5	<0.5	1.3	0.9	0.8	–
Rb	INAA	10	18	22	20	18	25	22	18	20	21	–
Sr	F-ICPES	1	684	665	755	707	601	615	641	1706	1666	–
Y	F-ICPES	1	21	24	22	23	21	21	19	13	13	–
Zr	F-ICPES	1	163	197	174	219	164	191	117	133	133	–
Ag	TD-ICPES	0.4	<0.4	<0.4	<0.4	<0.4	<0.4	<0.4	<0.4	<0.4	<0.4	–
Cd	TD-ICPES	0.5	<0.5	<0.5	<0.5	0.8	<0.5	0.5	<0.5	<0.5	<0.5	–
Sb	INAA	0.1	<0.1	0.1	0.1	0.1	<0.1	<0.1	<0.1	<0.1	<0.1	–
Cs	INAA	0.2	2.5	1.1	4.4	1.9	0.4	0.8	0.4	0.5	0.5	–
Ba	F-ICPES	1	344	365	362	396	360	390	338	506	498	–
La	INAA	0.1	20.1	20.9	20.4	21.5	17.7	21.6	13.3	29.6	29.3	–
Ce	INAA	1	37	42	44	38	35	40	27	53	55	–
Nd	INAA	1	19	21	22	20	17	19	12	30	29	–
Sm	INAA	0.01	3.85	4.46	4.48	3.86	3.50	3.97	2.80	4.58	4.65	–
Eu	INAA	0.05	1.30	1.37	1.41	1.25	1.16	1.26	0.99	1.46	1.40	–
Tb	INAA	0.1	0.6	0.7	0.7	0.6	0.6	0.6	0.5	0.5	0.5	–
Yb	INAA	0.05	1.68	1.83	1.80	1.71	1.63	1.78	1.72	1.00	1.06	–
Lu	INAA	0.01	0.25	0.26	0.26	0.25	0.24	0.26	0.24	0.15	0.15	–
Hf	INAA	0.2	3.2	3.9	3.6	3.5	3.0	3.5	2.5	3.0	3.2	–
Ta	INAA	0.3	0.6	0.3	0.5	0.7	0.5	0.8	0.6	0.3	0.4	–
Au	INAA	2	<2	<2	<2	<2	<2	2	<2	<2	<2	–
Hg	INAA	1	<1	<1	<1	<1	<1	<1	<1	<1	<1	–
Pb	TD-ICPES	5	<5	<5	<5	8	<5	6	6	8	8	–
Bi	TD-ICPES	5	<5	<5	<5	6	<5	<5	<5	<5	<5	–
Th	INAA	0.1	1.8	2	2	1.8	1.9	2.0	1.4	2.9	2.9	–
U	INAA	0.1	0.6	0.6	0.4	0.4	0.6	0.6	0.4	0.9	0.9	–

observation is corroborated by whole-rock chemical analyses (see next section). X-ray diffraction analyses of precipitates collected from Tuxpan shield lavas in the spring area (Table 2) also confirm our petrographic results. Precipitates consist mostly of amorphous silica (85–100%) followed by goethite (up to 15%), calcite (up to 11%) and minor amounts of sepiolite (up to 3%). In comparison, a shale sample from the Cretaceous marine sequence underlying the Tuxpan shield lava flows and collected uphill from the W margin of the Tuxpan River (along the road from Agua Blanca to Las Anonas) yielded almost equal amounts of smectite (33.9%) and calcite (32.7%) in addition to minor amounts of plagioclase (12.8%), clinoptilolite (8.3%), quartz (7.1%), mica (3.0%), and K-feldspar (2.2%). It seems that groundwaters incorporated HCO_3-ions enhancing their ability to corrode Mg–Fe-bearing silicates such as olivine contained in the overlying Tuxpan shield lava flows.

Sample 9705 from Molcajete scoria cone is similar in composition to Tuxpan shield samples. Idiomorphic millimeter-sized olivine crystals with Cr-spinel inclusions occur together with augite in a glassy matrix with feldspar microlites. In strong contrast, Zacapendo samples are characterized by orthopyroxene and clinopyroxene phenocrysts set in a glassy matrix that includes pyroxene and feldspar microlites. Clinopyroxene phenocrysts either occur as single individuals or in glomeroporphyritic clusters. In addition, hornblende "ghosts" (totally altered to oxides) as well as millimeter-sized quartz xenocrysts were observed. These petrographic observations on Zacapendo thin sections basically confirm those described earlier by Blatter and Carmichael (1998).

4.2. Geochemistry of volcanic rocks

Major and trace element analyses of samples from the Tuxpan shield, Molcajete, and Zacapendo volcanoes are listed in Table 3. Several samples from the Tuxpan shield were collected at different localities (proximal and distal) in order to determine compositional variability and genetic relationships. A few additional analyzed samples from the Zacapendo and Molcajete scoria cones are included for comparison.

Whole-rock silica (SiO_2) contents of the Tuxpan shield range narrowly from 53.1 to 54.6 wt.%. Molcajete displays a slightly higher silica content (55%) while two samples from Zacapendo are more siliceous (59.3% to 59.6%). The rocks are classified based on SiO_2 and total alkali (Na_2O+K_2O) contents (Fig. 7). All of the analyzed rocks are subalkaline. According to this scheme, the Tuxpan shield and Molcajete cone produced calc–alkaline basaltic andesites while Zacapendo erupted high-silica andesites.

Comparison of SiO_2 and MgO contents in distal lavas and proximal samples (dike and scoria) of the Tuxpan shield indicate a clear trend. Distal lavas have the lowest SiO_2 contents while proximal samples are more silicic. Surprisingly, MgO contents are highest in the most silicic proximal samples (MgO = 5.0 to 5.5%)

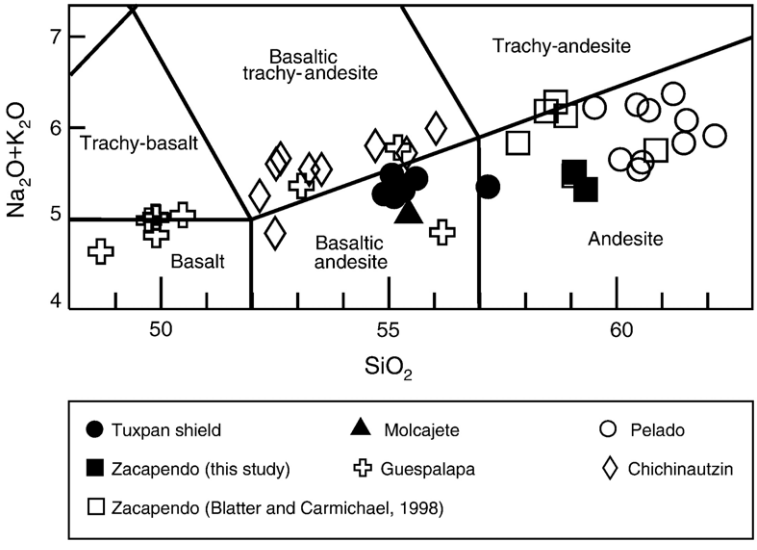

Fig. 7. Total alkalis (Na_2O+K_2O) plotted against silica (SiO_2) after Les Bas et al. (1986) for all analyzed Jungapeo area volcanic rocks. Analyses of samples from Pelado, Guespalapa, and Chichinautzin scoria cones in the Sierra Chichinautzin Volcanic Field near Mexico City (from Siebe et al., 2004) and additional samples from Zacapendo (from Blatter and Carmichael, 1998) are shown for reference. The dividing line separating alkali olivine basalts and tholeiites in Hawaii (MacDonald and Katsura, 1964) is also shown.

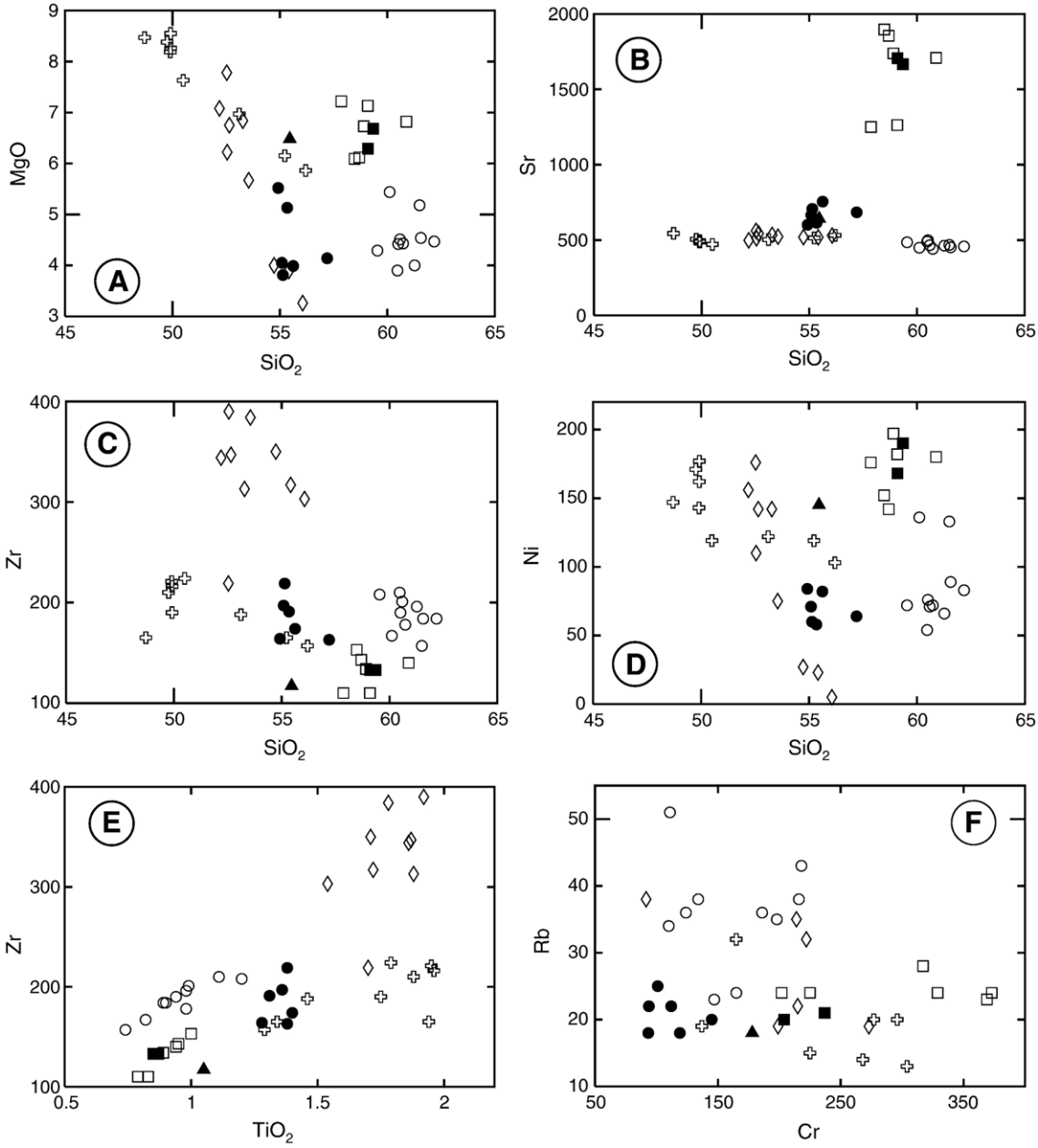

Fig. 8. Variation diagrams showing selected major (in wt.%) and minor elements (in ppm). Key symbols as in Fig. 7.

and lowest in the least silicic distal samples (MgO = 3.7–4.0%) (see Table 3 and Fig. 8A). This apparent contradiction is easily explained by the strong iddingsitization of the olivines observed in thin sections of distal samples. In these samples Mg has been leached out by low-temperature thermal waters replacing the olivines by Fe-oxides, silica, and carbonates (Fig. 6). Distal lavas also display high (1.6–2.3 wt.%) loss on ignition (LOI) values indicating the presence of hydrated glass and other secondary minerals (Table 3).

Different major and trace elements were plotted against silica as well as other elements (Figs. 7 and 8). Analyses of basaltic to andesitic samples from monogenetic Guespalapa, Chichinautzin, and Pelado scoria cones located within the Sierra Chichinautzin Volcanic Field south of Mexico City (Siebe et al., 2004) were included for comparison. From these plots it becomes clear that rocks from the Tuxpan shield and Molcajete bear many resemblances with rocks from the Sierra Chichinautzin. On the other hand, Zacapendo high-Si

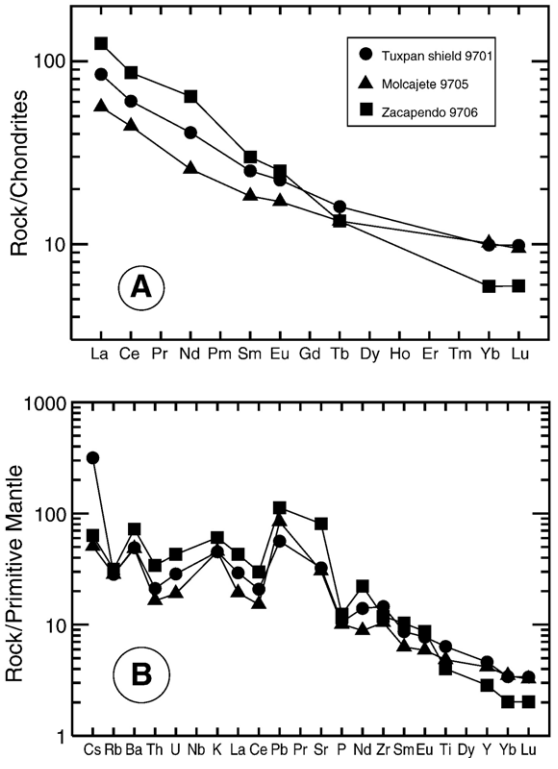

Fig. 9. (A) Chondrite-normalized (Sun and McDonough, 1989) REE compositions (in ppm) of analyzed volcanic rocks from the Jungapeo area. (B) Trace element abundances normalized to primitive mantle of analyzed volcanic rocks from the Jungapeo area. Primitive mantle values employed are from Sun and McDonough (1989).

andesites are quite unusual with extraordinarily high MgO, Sr, and Ni contents (Fig. 8A, B, and D, respectively). Although much more evolved than Tuxpan shield lavas (see also the Rare Earth element patterns and trace element distributions in Fig. 9), Zacapendo rocks are higher in certain compatible elements such as Mg and Ni. This indicates that Tuxpan shield compositions were not parental to Zacapendo lavas and therefore excludes a simple genetic relationship by crystal fractionation processes. This conclusion is quite striking, especially if one considers that both, the Tuxpan shield and Zacapendo lava flow are closely related in time and space and maybe even located on the same fault at a horizontal distance of less than 8 km (Fig. 1). Without getting into too many petrogenetic details (which would be beyond the scope this study), it can be said that chemical analyses of Tuxpan and Zacapendo lavas point toward a heterogeneous (enriched/depleted ± hydrated) lithospheric mantle source underneath this part of the TMVB. The detailed study of monogenetic volcanism in other parts of the TMVB (e.g. Sierra Chichinautzin) has lead to such a conclusion before (Siebe et al., 2004; Schaaf et al., 2005). The close spatial occurrence of monogenetic volcanoes, whose origin can be chemically traced back to different deep sources in the mantle, implies rapid ascent along extensional faults of relatively small batches of magma. Rapid ascent without stagnation in larger shallow magma chambers prevents the induction of high-temperature geothermal systems. From the above arguments, the occurrence of larger subvolcanic bodies of cooling magma seems unlikely underneath the Jungapeo area.

5. Geohydrology and visual characteristics of springs

The Tuxpan shield from which the majority of springs issue forms a broad cone having a radius from the summit to the west of more than 6 km. The area occupied by the Tuxpan shield is 92 km^2 (determined using a compensating polar planimeter on topographic maps). An accurate thickness of the shield is difficult to determine because the pre-existing topography is not known. None the less, the minimum volume of erupted products was crudely estimated to be 6.44 km^3 by multiplying the area covered by the shield (92 km^2) with an average thickness (70 m) determined by observations at lava flow margins along the Tuxpan River canyon.

The nearest meteorological station to Jungapeo is at Laguna del Fresno near Maravatío, about 55 km to the north. From 1992 to 2005, the average yearly rainfall for 12 years at this station is 700 ± 127 mm/yr (±18%) (see also Fig. 10 for more details). Using the computed value for average rainfall and a catchment area for rainfall on the shield of 92 km^2, the annual volume of water recharged into the shield is about $6.5 \pm 1.3 \times 10^8$ l/yr. This recharge water percolates into the permeable basaltic andesite lava flows and flow breccias of the shield and flows radially away from the summit down hydrologic gradient. Much of this water emerges as springs around the western flank of the shield and most of the springs consist of the CO_2-rich thermal waters along the Río Tuxpan in the Jungapeo area. The estimated yearly discharge volume of these thermal springs is roughly 6×10^8 l/yr based on flow measurements obtained in March 1997 (Table 4). The discharge measurements were measured with a bucket and stopwatch in most cases having an error of ±10%, but do not account for seasonal variations. Yet it seems apparent that much of the water recharged on the shield can be accounted for in the discharge from the springs.

Many of the springs are unimproved issuing from natural or crudely constructed pools in basaltic andesite

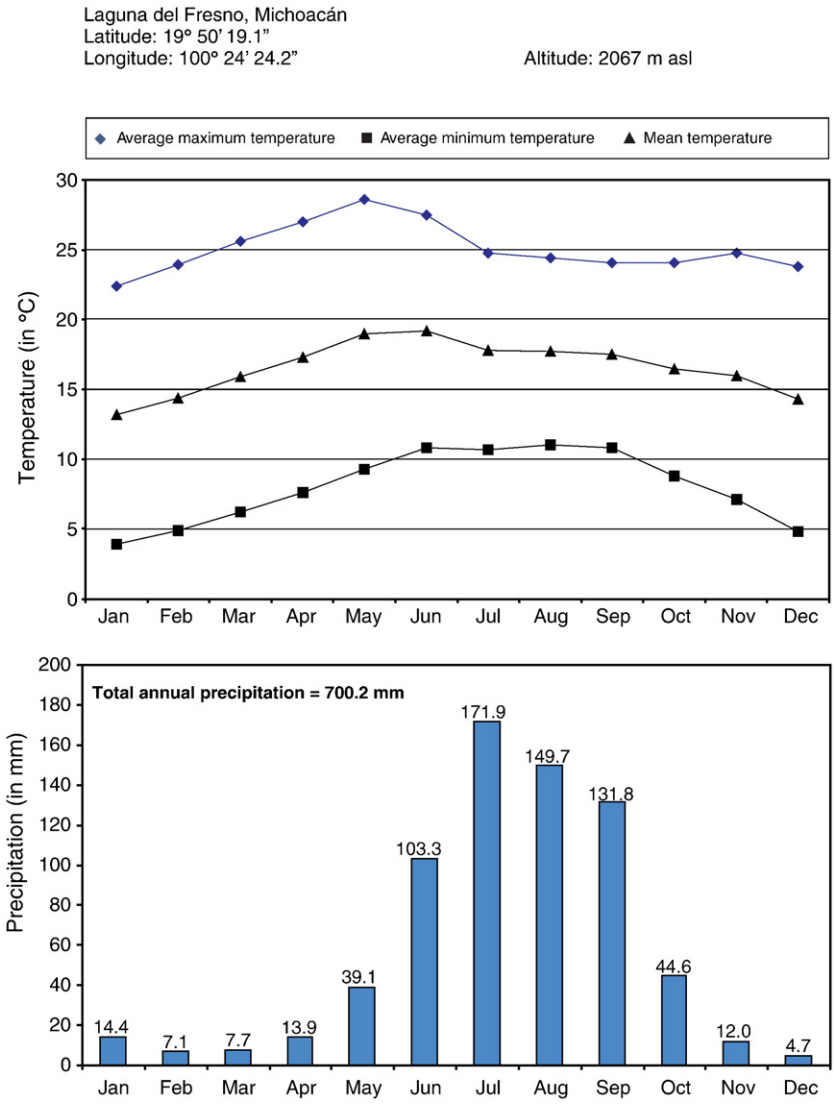

Fig. 10. Average monthly precipitation and average monthly minimum, mean, and maximum temperatures for the period 1992–2005 as measured at Laguna del Fresno, located 7 km south of Maravatío and 55 km N of Jungapeo.

rocks along the eastern canyon wall (Fig. 11A). However, the springs at SJP, AB, EA, and CA are improved with emergence points protected by grottos and concrete boxes, and flow directed through pipes into various types of commercialized and private pools (Fig. 11B to D). The dominating characteristics of the thermal waters are their moderate temperatures (28 to 32 °C), relatively high flow rates, effervescence of CO_2 gas, clarity at emergence, and precipitation of hydrous iron oxides around pool margins and channel ways. Waters contained in larger pools become pale green to orange as dissolved ferrous iron converts to coagulants of hydrated ferric oxides (Fig. 11A, B, and C). Additional precipitates of carbonate and silica form with the Fe-oxides as the waters cascade toward the Río Tuxpan. An old leaflet distributed to tourists several decades ago for the purpose of advertising the medical benefits of the mineral waters, included a paragraph claiming that the elevated levels of radioactivity of the waters would also contribute to their soothing effects. As a result, we measured radioactivity with a Geiger–Müller detector but found that the spring waters and surrounding rocks are not particularly radioactive and are indistinguishable from the regional background noise.

An analysis of the dried Fe-rich coagulant from the main pool at Agua Blanca (Table 3) reveals about 65% Fe_2O_3, 14% SiO_2, 4% CaO, and 4% P_2O_5 (by weight). X-ray diffraction analysis of this sample shows that it is

Table 4
Field and isotope data for CO_2-rich spring waters, Jungapeo area, Mexico[a]

Sample	Location	Latitude	Longitude	Altitude (m)	Date	Temperature (°C)	Field pH	Flow (l/min)	$\delta^{18}O$ (‰)	δD (‰)	^3H (TU)	Rock type
MVT-3	San José Purúa[b]	19°29′19.8″	100°29′31.6″	1455	24/06/1995	31.8	6.2	nd	−8.7	−67	0.82±0.09	Basaltic andesite
MVT-27	San José Purúa[b]	19°29′19.8″	100°29′31.6″	1455	03/03/1997	32.4	6.0	150	−9.2	−61	nd	Basaltic andesite
MVT-4	Agua Blanca; resort[c]	19°28′41.8″	100°29′40.1″		25/06/1995	31.0	6.3	nd	−8.7	−66	1.33±0.09	Basaltic andesite
MVT-25	Agua Blanca; source[d]	19°28′47.4″	100°29′34.2″	1340	02/03/1997	29.7	6.0	>200	−9.2	−65	1.22±0.09	Basaltic andesite
EP-9403	El Puente[e]	19°28′45.9″	100°29′38.1″	1335	01/03/1994	29.1	6.0	nd	nd	nd	nd	Basaltic andesite
MVT-22	Agua Amarilla[f]	19°29′06.7″	100°29′48.3″	1350	01/03/1997	30.6	6.2	300	−9.3	−63	nd	Basaltic andesite
MVT-23	El Tular[g]	19°28′09.0″	100°29′32.1″	1315	02/03/1997	29.2	6.0	60	−9.4	−63	0.33±0.09	Basaltic andesite
MVT-24	Cañada Azul; pool[h]	19°28′32.3″	100°29′32.3″	1355	02/03/1997	26.0	6.0	≥10	−9.3	−63	1.21±0.09	Basaltic andesite
MVT-26	El Aguacate; pool[i]	19°29′09.7″	100°29′50.4″	1300	02/03/1997	31.8	6.5	15	−8.8	−64	1.78±0.09	Limestone
MVT-28	Varelas[j]	19°30′22″	100°29′39″	1475	03/03/1997	29.8	5.8	250	−9.6	−68	nd	Basaltic andesite
MVT-29	El Sauz[k]	19°30′06″	100°29′34″	1500	03/03/1997	28.3	5.7	80	−9.6	−62	nd	Basaltic andesite
MVT-30	El Gauyabo[l]	19°30′06″	100°29′28″	1510	03/03/1997	29.4	5.5	60	−9.5	−61	nd	Basaltic andesite
MVT-31	El Concreto[m]				03/03/1997	24.5	6.8	120	−9.5	−64	2.09±0.11	Basaltic andesite
MVT-32	El Zapote[n]	19°30′03″	100°29′24″	1525	03/03/1997	30.2	6.0	15	−9.3	−64	0.69±0.09	Basaltic andesite

[a] Temperature by probe; pH by indicator strips; flow by visual estimate; oxygen-18 error=±0.25‰; deuterium error=±1‰; tritium error is shown in table.
[b] From pool in grotto constructed beneath cliff of lava; free gas; Fe-oxide precipitate; other springs on property, some possibly warmer.
[c] From inlet pipe to main pool; considerable gas discharge and Fe-oxide precipitate.
[d] From beneath concrete box around source in ravine of lava and flow breccia; large amount of gas; Fe-oxide precipitate.
[e] From abandoned pool just upstream of bridge on road; minor gas; minor Fe-oxide precipitate.
[f] From source at rock pool in colluvium about 6 m below contact with lava; free gas; considerable Fe-oxide precipitate.
[g] From source above rock pool in lava talus; free gas; considerable Fe-oxide precipitate.
[h] From source in concrete box in lava; free gas; considerable Fe-oxide precipitate.
[i] From terrace gravel and colluvium on southwest side of Rio Tuxpan; diluted with river water or groundwater; minor gas; faint H_2S odor.
[j] From source at rock pool in lava; very minor gas; considerable Fe-oxide precipitate.
[k] From rock pool in colluvium beneath lava; no gas; minor Fe-oxide precipitate.
[l] From rock pool in colluvium beneath lava; free gas; minor Fe-oxide precipitate.
[m] From concrete box in colluvium; collected as cold background sample.
[n] From rock pool in colluvium beneath contact with lava; free gas; minor Fe-oxide precipitate.

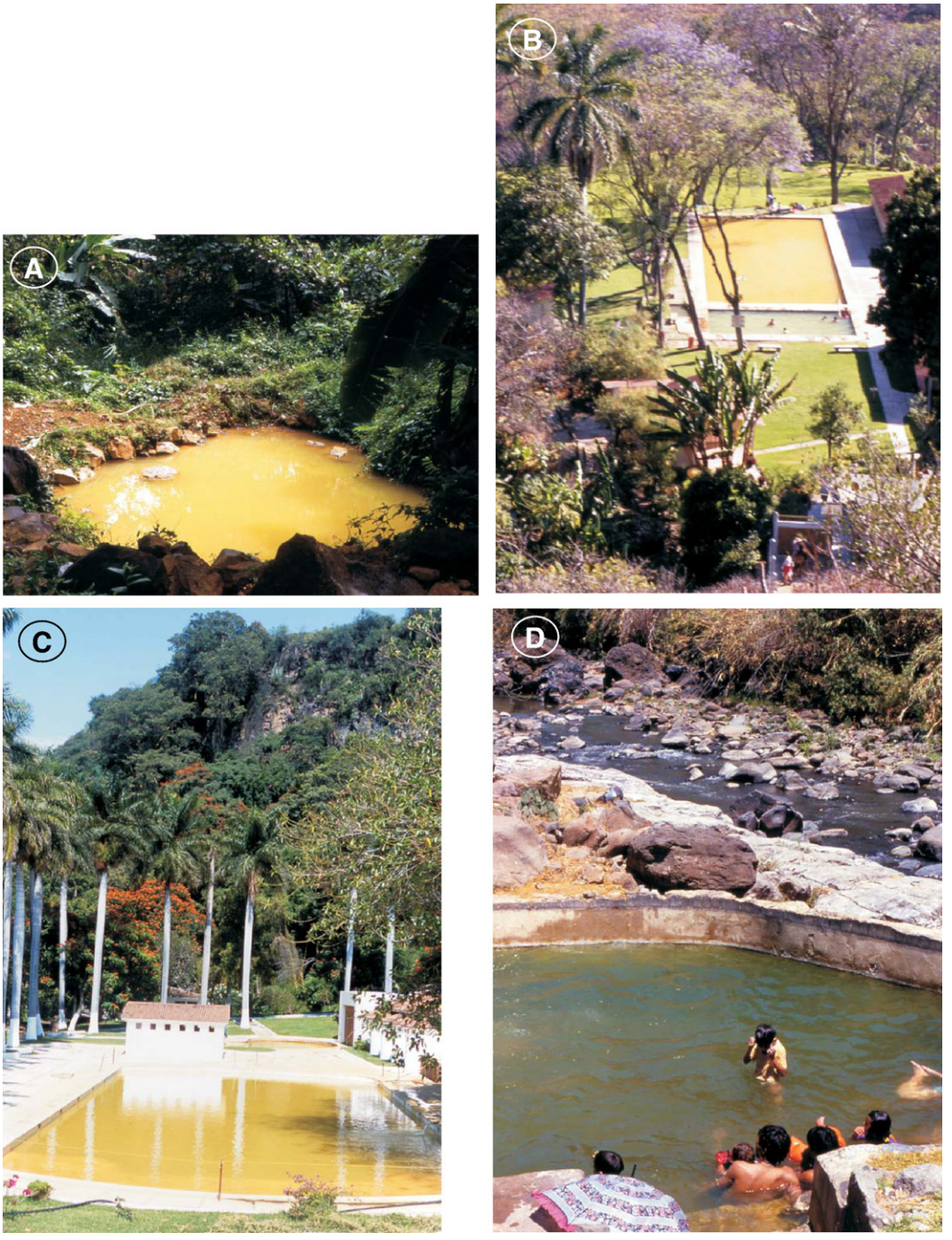

Fig. 11. (A) Small bathing pool at El Tular mineral spring near Jungapeo. Note characteristic yellowish color due to Fe-mineral precipitation. Photo taken August 1992. (B) Agua Blanca resort with swimming pools. Mineral water is conducted in a tube from a spring located 100 m behind the viewer to the smaller (greenish) pool and from there to the larger (yellow) pool. Differences in color are due to increasing amounts of precipitates at water temperatures ranging from 31 °C (green pool) to 28 °C (yellow pool). Photo taken February 28, 2004. (C) San José Purúa resort. Note characteristic yellow color due to Fe-mineral precipitation. Photo taken October 28, 2005. (D) El Aguacate mineral spring located on the west margin of the Río Tuxpan. During the rainy season (June–September) this spring is often inundated by the torrent of the river. Photo taken April 1994. All photos by Claus Siebe.

Table 5
Selected major and trace element analyses of CO_2-rich waters from Jungapeo area, Mexico (values in ppm unless otherwise noted; na means not analyzed or measured). A complete tabulation of our 85 major element analyses of the Jungapeo waters can be obtained from the first author

Sample	Location	Date (mm/dd/yyyy)	Analyst	Temperature (°C)	pH (lab)	SiO_2	Na	K	Li	Ca	Mg	Fe	F	Cl	HCO_3	SO_4	B	TDS
SJP-9408	San José Purúa	11/08/1994	Armienta	31.7	6.77	114	235	21.4	na	114	84.9	7.34	na	141	1310	10.7	7.07	1994
SJP-9410	San José Purúa	09/10/1994	Armienta	32.3	6.73	117	279	31.4	na	111	80.1	7.17	0.56	145	1285	10.4	6.86	2073
MVT-3	San José Purúa	24/06/1995	Counce	31.8	6.85	143	257	23.1	1.39	120	92.2	7.33	0.21	148	1195	10.2	7.53	2008
MVT-27	San José Purúa	03/03/1997	Counce	32.4	7.82	136	243	22.3	1.36	109	81.8	6.11	0.19	151	1205	9.63	8.10	1975
AB-9408	Agua Blanca	11/08/1994	Armienta	29.5	6.34	107	225	17.7	na	115	75.7	7.83	na	139	1240	12.9	7.04	1876
AB-9410	Agua Blanca	08/10/1994	Armienta	30.0	6.77	96.1	245	24.8	na	111	79.2	7.86	0.347	130	1065	13.3	5.66	1778
MVT-4	Agua Blanca	25/06/1995	Counce	31.0	6.82	130	218	19.1	1.10	110	84.5	7.23	0.30	134	1095	12.7	7.00	1822
MVT-25	Agua Blanca	02/03/1997	Counce	29.7	6.99	127	219	20.5	1.21	107	78.6	6.87	0.23	139	1110	13.5	7.61	1832
EP-9406	El Puente	18/06/1994	Armienta	28.9	6.19	102	175	19	na	109	66.0	na	na	105	1030	20.3	8.26	1635
EP-9410	El Puente	08/10/1994	Armienta	29.1	6.57	70.2	194	17.7	na	96.2	73.4	7.38	0.45	105	1060	20.2	5.80	1650
AA-9408	Agua Amarilla	18/06/1994	Armienta	30.8	6.43	165	217	20.8	na	109	78.2	5.4	na	140	1175	20.0	6.01	1877
AA-9410	Agua Amarilla	08/10/1994	Armienta	30.8	6.8	86.9	228	17.3	na	105	77.4	4.36	0.32	125	1140	19.9	5.97	1810
MVT-22	Agua Amarilla	01/03/1997	Counce	30.6	7.21	129	212	19.6	1.15	105	81.7	4.86	0.27	128	1060	21	6.73	1772
ET-9408	El Tular	13/08/1994	Armienta	28.4	6.37	104	182	17.6	na	96.7	67.8	8.0	na	107	937	3.15	5.59	1529
ET-9410	El Tular	08/10/1994	Armienta	29.7	6.51	72.5	196	23.2	na	102	64.9	6.89	0.35	105	1005	2.76	5.94	1585
MVT-23	El Tular	02/03/1997	Counce	29.2	6.85	123	176	17.3	0.93	90.2	64.8	5.45	0.27	110	929	3.75	6.36	1530
CA-9408	Cañada Azul	11/08/1994	Armienta	27.0	6.09	93.6	146	14.5	na	79.6	58.0	4.74	na	84.5	770	12	4.63	1268
CA-9410	Cañada Azul	08/10/1994	Armienta	27.3	6.21	91.6	161	20.8	na	78.6	56.3	4.94	0.4	85	831	11.9	4.32	1346
MVT-24	Cañada Azul	02/03/1997	Counce	26.0	6.89	115	144	15.1	0.75	79.6	60.7	4.16	0.25	90.8	792	11.7	4.76	1323
EA-9404	El Aguacate	01/04/1994	Armienta	34.7	6.69	96.5	1425	60	na	72.8	50.4	0.86	0.65	660	2290	98.3	29.1	4784
EA-9406	El Aguacate	18/06/1994	Armienta	33.8	6.48	70.6	750	35	na	77.3	47.1	na	na	500	1570	80.7	24.1	3155
MVT-26	El Aguacate	02/03/1997	Counce	31.8	7.92	86.5	826	30.6	2.03	88.5	32.7	0.10	0.44	446	1877	96.2	19.7	3512
VA-9408	Varelas	12/08/1994	Armienta	29.6	6.45	103	118	11.0	na	109	23.2	5.91	na	42.6	755	16.2	1.74	1148
VA-9410	Varelas	09/10/1994	Armienta	30.1	6.38	95.1	137	13.5	na	66.8	48.8	5.2	0.35	43.0	731	16.4	3.84	1161
MVT-28	Varelas	03/03/1997	Counce	29.8	6.96	126	112	11.5	0.47	63.0	45.1	4.86	0.30	42.8	674	15.2	2.29	1099
ES-9408	El Sauz	12/08/1994	Armienta	28.1	6.48	99.3	88.6	8.74	na	48.3	40.9	4.39	na	27.1	523	19.9	1.33	862
ES-9410	El Sauz	09/10/1994	Armienta	28.8	6.45	103	99.6	12.9	na	47.1	40.5	3.93	0.45	30.0	545	20.4	1.67	905
MVT-29	El Sauz	03/03/1997	Counce	28.3	7.51	118	83.4	9.31	0.35	46.2	38.4	3.90	0.34	28.1	509	20.1	1.54	860
EG-9410	El Gauyabo	09/10/1994	Armienta	30.0	6.11	74.0	206	13.9	na	73.2	61.9	7.26	0.32	49.5	827	7.67	2.44	1323
MVT-30	El Gauyabo	03/03/1997	Counce	29.4	7.44	126	115	12.5	0.51	70.2	60.1	5.90	0.28	48.3	765	8.49	2.66	1217
MVT-31	El Concreto	03/03/1997	Counce	24.5	8.19	105	60.6	8.66	0.23	39.5	47.7	0.04	0.33	29.5	445	41.7	1.30	757
EZ-9408	El Zapote	12/08/1994	Armienta	29.1	6.47	106	136	15.1	na	84.6	71.9	6.23	na	63.0	965	10.3	3.03	1412
EZ-9410	El Zapote	08/10/1994	Armienta	29.8	6.50	93.2	148	16.1	na	77.6	76.2	5.22	0.37	62.5	918	10.8	2.93	1411
MVT-32	El Zapote	03/03/1997	Counce	30.2	7.77	131	131	14.3	0.59	80.3	72.3	5.29	0.24	61.8	864	10.7	3.21	1378

Table 6
Trace element analyses of thermal waters from Jungapeo area, Mexico (values in ppm unless otherwise noted). Footnotes same as Table 4[a]

Sample	Location	Analyst	Temperature (°C)	Al	As	Ba	Br	Cs	Cu	I	Mn	NH_4	Ni	NO_3	PO_4	Rb	Sr	V
SJP-9408	San José Purúa	Armienta	31.7	0.1	<0.001	na	0.3	na	na	na	na	na	na	2.4	<0.05	na	0.75	na
MVT-3	San José Purúa	Counce	31.8	0.12	0.002	0.29	0.31	0.21	<0.002	<0.01	0.36	1.02	0.009	0.14	<0.05	0.15	1.02	0.002
MVT-27	San José Purúa	Counce	32.4	0.38	0.0020	0.30	0.25	0.14	0.002	0.010	0.33	1.02	<0.002	0.04	<0.05	0.13	0.98	0.002
AB-9408	Agua Blanca	Armienta	29.5	0.05	0.001	na	0.27	na	na	na	na	na	na	<0.02	na	na	0.5	na
MVT-4	Agua Blanca	Counce	31.0	0.17	0.001	0.28	0.27	0.20	<0.002	<0.05	0.31	1.16	0.003	0.04	<0.05	0.11	0.93	<0.002
MVT-25	Agua Blanca	Counce	29.7	0.40	0.0032	0.30	0.20	0.18	<0.002	0.008	0.29	0.66	0.007	<0.02	<0.05	0.13	0.97	0.002
AA-9408	Agua Amarilla	Armienta	30.8	0.06	<0.001	na	0.26	na	na	na	na	na	na	0.2	<0.05	na	0.6	na
MVT-22	Agua Amarilla	Counce	30.6	0.41	0.0013	0.27	0.18	0.18	0.003	<0.005	0.37	0.89	0.006	0.03	<0.05	0.15	0.93	<0.002
MVT-23	El Tular	Counce	29.2	0.33	0.0006	0.23	0.19	0.13	0.002	0.005	0.28	0.76	<0.002	<0.02	<0.05	0.11	0.77	<0.002
MVT-24	Cañada Azul	Counce	26.0	0.23	0.0007	0.18	0.13	0.15	<0.002	0.007	0.24	0.57	<0.002	2.15	<0.05	0.11	0.65	0.004
MVT-26	El Aguacate	Counce	31.8	0.33	0.037	0.11	0.70	0.13	0.009	0.017	0.18	0.62	<0.002	2.29	<0.05	0.12	1.76	0.004
VA-9408	Varelas	Armienta	29.6	0.1	<0.001	na	0.05	na	na	na	na	na	na	0.78	<0.05	na	0.39	na
MVT-28	Varelas	Counce	29.8	0.34	0.0014	0.12	0.11	0.092	<0.002	0.017	0.24	0.46	<0.002	0.02	<0.05	0.069	0.52	0.003
MVT-29	El Sauz	Counce	28.3	0.20	0.0036	0.07	0.05	0.062	0.002	0.009	0.18	0.29	0.006	0.04	<0.05	0.049	0.36	0.002
MVT-30	El Gauyabo	Counce	29.4	0.22	0.0019	0.12	0.09	0.089	0.036	0.006	0.32	0.38	0.054	0.11	<0.05	0.074	0.59	0.002
MVT-31	El Concreto	Counce	24.5	0.13	0.0010	0.02	0.04	0.015	0.003	<0.005	0.002	0.06	0.006	7.10	0.6	0.036	0.34	0.033
EZ-9408	El Zapote	Armienta	29.1	0.1	<0.001	na	<0.02	na	na	na	na	na	na	2.2	<0.05	na	0.48	na
MVT-32	El Zapote	Counce	30.2	0.28	0.0030	0.12	0.15	0.093	<0.002	<0.005	0.35	0.32	0.010	1.09	<0.05	0.090	0.66	0.013

[a] All samples were at or below detection limits for the following elements: Ag ≤ 0.002; Be < 0.002; Cd < 0.001; Co < 0.002; Cr < 0.002; Hg < 0.0002; Mo ≤ 0.002; NO_2 ≤ 0.02; Pb ≤ 0.002; Sb < 0.0002; Se ≤ 0.0002; S_2O_3 < 0.01; Ti ≤ 0.01; Zn ≤ 0.02.

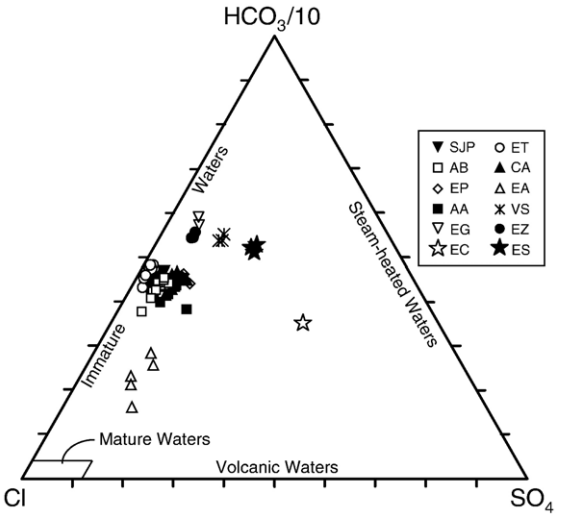

Fig. 12. Triangular plot of $HCO_3/10$-SO_4-Cl for waters of the Jungapeo area, Mexico. The plot is modified from Giggenbach (1992) to provide more definition for bicarbonate-rich waters.

amorphous. Assuming that CaO is actually $CaCO_3$, carbonate probably makes up 7% of the sample. Ferric oxides, calcite, and opaline silica can be found as cements and coatings in the basaltic rocks near the spring areas, especially in the flow breccias. On the western margin of the shield south of San José Purúa abundant fragments of opaline silica and calcite with coatings of Fe-rich oxides are found in the cultivated surface of the basalt suggesting that thermal springs may have once discharged at higher elevations. Road cuts through soils into the underlying basalt commonly reveal deposits of caliche as much as 0.5 m thick formed at the base of the soil horizon. X-ray diffraction analyses of three samples of these old deposits (Table 2) verify that they consist primarily of opal-A to opal-CT, goethite and calcite. One sample possibly contains a small amount of sepiolite ($Mg_4Si_6O_{15}(OH)_2(H_2O)_6$).

6. Water geochemistry

6.1. Chemistry and mixing relations

Selected major element analyses of Jungapeo waters are presented in Table 5 while all trace element data of waters are listed in Table 6. From a geothermal perspective, Jungapeo mineral waters are chemically characterized by moderate SiO_2, Ca+Mg nearly equal to Na+K, high HCO_3, moderate to low Cl, and low F and SO_4. With respect to key geothermal trace elements, B is rather high, Li is moderate, while Br and As are quite low. In contrast, Fe+Mn is exceptionally high (the iron in solution is Fe^{2+}). Thus, Jungapeo mineral waters do not have the typical chemical composition of high-temperature geothermal reservoir fluids or derivative hot springs (Goff and Janik, 2000). Instead, the Jungapeo fluids resemble soda spring waters from other parts of the world that may or may not be associated with high- to moderate-temperature geothermal activity (e.g. Barnes et al., 1973; Pauwels et al., 1997; Marques et al., 2004; Inguaggiato et al., 2005; Choi et al., 2005).

Waters from El Aguacate (EA) are somewhat different from those mentioned above. Waters from EA have much more Na+K, Cl, B, and As but much less Ca+Mg and Fe+Mn than other Jungapeo fluids. As a result EA waters appear more geothermal in character than other Jungapeo fluids.

On a bicarbonate–chloride–sulfate ternary (Fig. 12), Jungapeo waters plot in the immature field of geothermal fluids as defined by Giggenbach (1992). Note that HCO_3/10 is used on this plot so that the Jungapeo data do not form a clump of points near the bicarbonate apex. Thus, El Aguacate (EA) fluids are the least immature whereas El Concreto (EC), El Gauyabo (EG), El Sauz (ES), El Zapote (EZ), and Varelas (VS) waters are the most immature. Two trends are discernible on the plot, both with EZ and EG waters at one end: a trend of relatively increasing

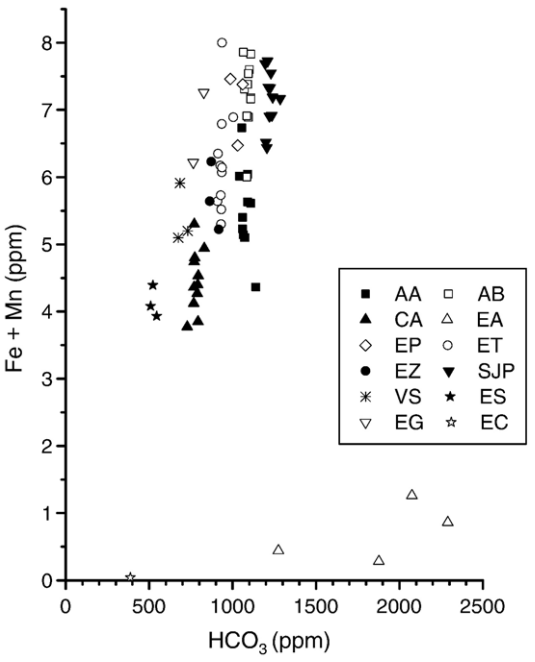

Fig. 13. Plot of (Fe+Mn) versus HCO_3 for waters of the Jungapeo area, Mexico. Most Jungapeo CO_2-rich waters form a single trend of high (Fe+Mn) with increasing bicarbonate. Water from El Aguacate spring is an exception containing much less (Fe+Mn) relative to bicarbonate.

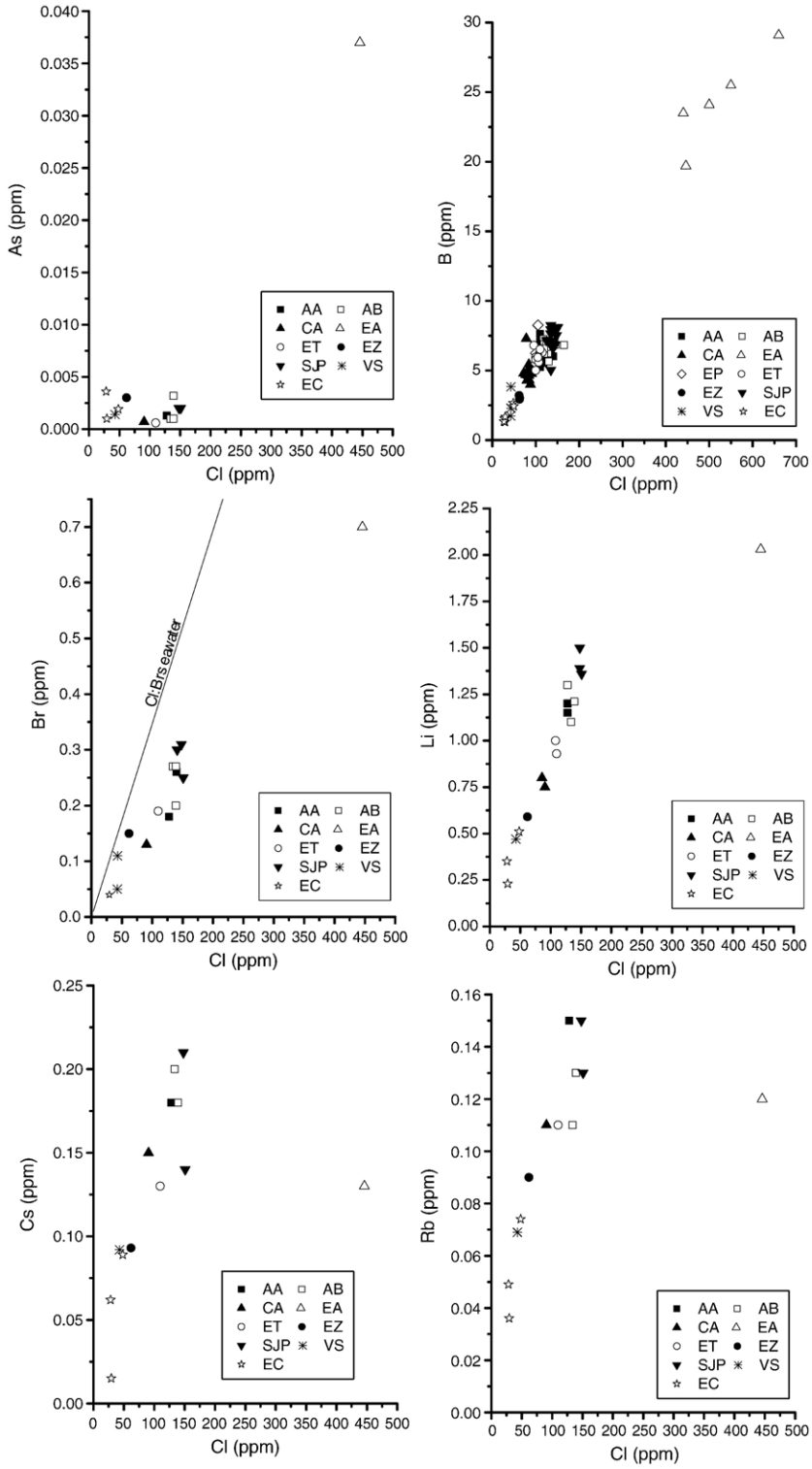

Fig. 14. Chloride variation diagrams using As, B, Br, Li, Cs, and Rb for waters of the Jungapeo area, Mexico. The Cl:Br line for seawater is calculated from Krauskopf (1979).

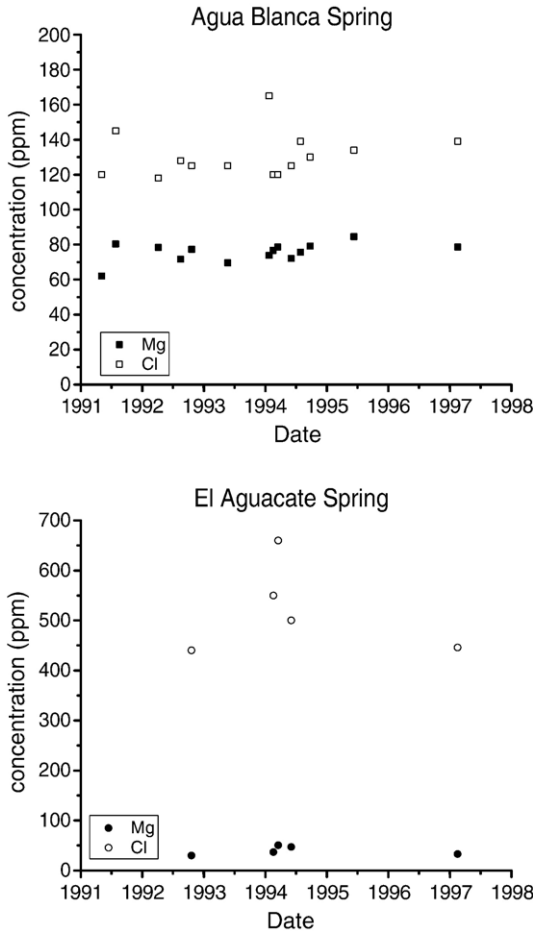

Fig. 15. Plot of Mg and Cl vs. sampling date for waters discharged from two springs in the Jungapeo area, Mexico.

chloride and decreasing bicarbonate toward mature waters and a trend of nearly constant Cl/HCO_3 but increasing sulfate toward the composition of EC water. The first trend suggests possible mixing between bicarbonate-rich groundwaters and a deep geothermal end-member, while the second trend indicates mixing of bicarbonate-rich groundwaters with a source of sulfate. In this case, EC water is also enhanced in nitrate and phosphate (Table 6) suggesting that the excess sulfate comes from agriculture (fertilizers such as ammonium sulfate, etc.) and not from a deep geothermal or volcanic source.

On the plot of Fig. 13, most Jungapeo fluids form a positive trend of highly increasing Fe+Mn with HCO_3. In contrast, EA waters form a completely separate trend of slightly increasing Fe+Mn with increasing HCO_3. The difference between the two trends is explained by differences in the host rocks. Waters with high Fe+Mn contents discharge from young glassy basaltic andesite rocks of the Tuxpan shield volcano whereas the EA waters (relatively low Fe+Mn) discharge from Cretaceous rocks W of the Río Tuxpan. Because they are glassy, the basaltic andesite rocks are highly reactive to bicarbonate-rich fluids and probably release their Fe+Mn rather easily, whereas the Cretaceous marls contain less Fe+Mn and release less of these constituents into solution. In this plot, the sample from EC (the sample with the least Cl) contains virtually no Fe+Mn suggesting that EC is composed of very young groundwater that interacts little with host rocks.

A plot of As versus Cl (Fig. 14) shows that most Jungapeo fluids plot as a cluster of very low As with respect to Cl. As does not increase as Cl increases. The exception is water from EA, which contains substantially higher As than other Jungapeo waters, although not nearly as high as As in most high-temperature geothermal fluids (see Table 3 of Goff and Janik, 2000).

The B versus Cl plot (Fig. 14) shows a very strong trend of increasing B with Cl. There are two segments

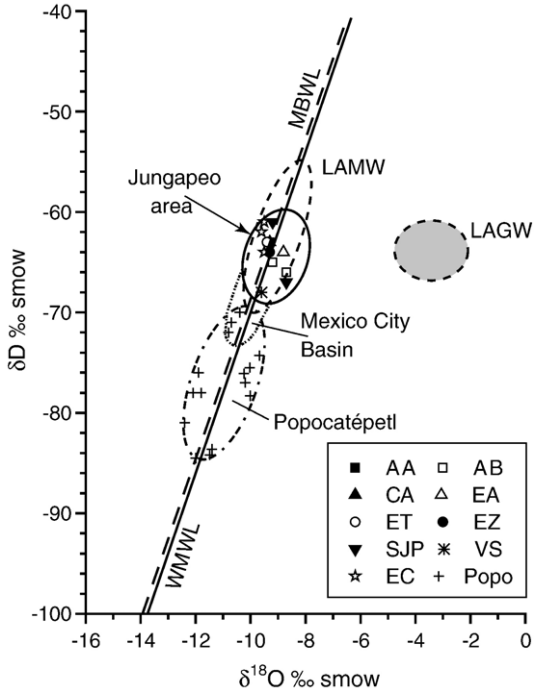

Fig. 16. Plot of ∂D versus $\partial^{18}O$ for waters of the Jungapeo area, Mexico (enclosed by solid line). WMWL=World Meteoric Water Line, $\partial D = 8\partial^{18}O + 10$ (Craig, 1961), MBWL=Mexico City Basin meteoric water line (dashed), $\partial D = 7.97\partial^{18}O + 11.03$ (Cortés et al., 1997), LAMW=oval showing range of Los Azufres meteoric waters and LAGW=range of Los Azufres pre-production geothermal well waters (Torres-Alvarado et al., 1995; Barragán et al., 2005). Additional ovals are also shown for the majority of Mexico City Basin meteoric waters as defined by the Gaussian distribution of data in Cortés et al. (1997, p. 374) and for the Popocatépetl data set of Inguaggiato et al. (2005). Plus symbols show data from Popocatépetl reported in Werner et al. (1997), and F. Goff (unpublished data).

on the trend: a concentrated segment (from a deeper source) for EA waters and a less concentrated segment (from a shallower source) for other Jungapeo waters. Within both segments, the data indicate that mixing with dilute water affects the chemistry of the two types of fluids. The Br–Cl plot (Fig. 14) mimics the B–Cl plot, defining one trend with a concentrated fluid represented by EA and a trend with less concentrated fluids represented by other Jungapeo fluids. The Jungapeo Br–Cl trend is not the same as the trend for seawater, which would imply that marine rocks are not the sole source of Br. Thus, Cl and Br may come from a variety of sources.

Plots of Li, Cs, and Rb vs. Cl (Fig. 14) all show the same pattern: a well-defined trend for less concentrated mineral fluids issuing from the basaltic andesite shield volcano and a different cation–chloride relationship for concentrated fluid represented by EA. EA waters flow through Cretaceous rocks on the W side of the Río Tuxpan. Possibly, Li, Cs, and Rb are more easily dissolved in carbonated waters circulating in glassy basaltic andesite rocks than in marine Cretaceous rocks. In contrast, rock type does not apparently affect the relative solubility of B and Br.

Fig. 15 compares concentration vs. sampling date for two constituents of different chemical behavior (Cl and Mg) from the two types of mineral water: less concentrated fluid represented by Agua Blanca spring and the more concentrated water of El Aguacate spring. Chloride is the more conservative (soluble) component while Mg is a less conservative component, partially controlled by carbonate solubility. We obtained 14 water samples from AB during the 6-year period from early 1991 to early 1997. Allowing that some of the variations are due to analytical errors, we observe that there are fluctuations in chemistry that probably represent seasonal dilution of mineral water with dilute groundwater and/or rainwater. Thus, in very early 1994, dry conditions in the area caused the Cl content of AB water to rise to levels of roughly 170 ppm but wet conditions commencing in April caused a reduction of Cl in AB water to more typical Cl values of roughly 130 ppm. Note that Mg content apparently behaves independent of Cl concentration and this independent behavior is evident in all springs. Only five samples comprise the EA data set (Fig. 15) but Cl content is positively correlated with temperature. Again, climate variations related to wet and dry seasons apparently affect the concentration of Cl in EA. Mg is less affected by climate than Cl.

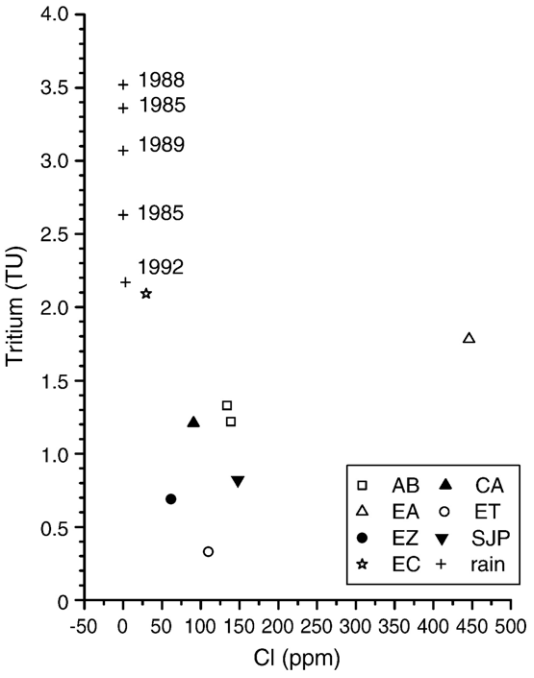

Fig. 17. Plot of ^{3}H versus Cl for waters of the Jungapeo area, Mexico. Rain data from 1985 to 1992 are from Goff et al. (1987), Janik et al. (1992) and Goff and McMurtry (2000).

6.2. Recharge to system

The plot of deuterium vs. oxygen-18 (Fig. 16) shows that the CO_2-rich thermal waters of the Jungapeo region form a cluster of points straddling the World Meteoric Water Line (WMWL, Craig, 1961) and the Mexico City Basin meteoric water line (MBWL, Cortés et al., 1997). Thus, Jungapeo thermal waters are recharged by precipitation of local meteoric water as indicated by our recharge–discharge measurements in Section 5. Cold water from El Concreto shows that background water and thermal waters are essentially identical in isotopic composition indicating that the Tuxpan shield is the recharge area for most springs. El Aguacate, the only spring discharging on the W side of the Río Tuxpan, has similar isotope composition to the rest of the springs. Thus, El Aguacate is also composed mostly of meteoric water from a similar local source even though water from this spring is substantially more concentrated in chloride than the others (see above).

For comparisons, the dashed ovals outline the areas of cold meteoric waters in the Los Azufres geothermal area (Torres-Alvarado et al., 1995), only 50 km NW of Jungapeo, for the majority of cold meteoric waters in the Mexico City Basin (Cortés et al., 1997), and for a small group of cold meteoric waters collected from the region around Popocatépetl Volcano (Inguaggiato et al., 2005)

Table 7
Gas analyses from selected bicarbonate-rich waters, Jungapeo, Mexico (values in mol%, unless noted)[a]

Sample #	Description	Date (mm/dd/yyyy)	Temperature (°C)	H_2	Ar	O_2	N_2	CH_4	C_2H_6	CO	CO_2	NH_3	H_2S	Total	$\delta^{13}C$–CO_2 (‰ PDB)
MVT-3	San José Purúa Spring, gazebo with Virgin	24/06/1995	31.8	<0.0003	0.0159	0.3325	1.0476	0.00376	<0.0003	<0.0002	98.61	0.00128	<0.001	100.01	−6.7*
MVT-27	San José Purúa Spring, gazebo with Virgin	03/03/1997	32.4	<0.001	0.0781	2.0412	7.2992	<0.002	<0.002	<0.001	90.59	<0.001	<0.00004	100.01	
MVT-4	Agua Blanca Spring, pipe in concrete box @ source	25/06/1995	31.0	<0.00004	0.0045	0.0195	0.1875	0.00865	<0.00004	<0.00002	99.78	0.00086	<0.001	100.00	−7.2
MVT-25	Agua Blanca Spring, pipe in concrete box @ source	02/03/1997	29.7	<0.00005	0.0037	0.0132	0.174	0.0085	<0.0001	<0.00005	99.8	<0.0005	<0.00001	100.00	−7.0
MVT-22b	Agua Amarilla Spring, from concrete box	01/03/1997	30.6	<0.002	0.1127	2.8331	11.5492	<0.003	<0.003	<0.002	85.55	<0.002	<0.00005	100.05	
MVT-23	El Tular Spring	02/03/1997	29.2	<0.0002	0.0274	0.1039	1.2715	0.01252	<0.0003	<0.0002	98.59	<0.0005	<0.00002	100.01	−6.8
MVT-24	Cañada Azul Spring, from concrete box	02/03/1997	26.0	<0.0002	0.0167	0.276	1.0592	0.00666	<0.0003	<0.0002	98.64	<0.0006	<0.00002	100.00	−7.0*
MVT-26b	El Aguacate Spring	02/03/1997	31.8	<0.0005	0.0504	1.2426	3.9409	<0.001	<0.001	<0.0005	94.8	<0.001	<0.00003	100.03	−6.8
MVT-30	El Guayabo Spring	03/03/1997	29.4	<0.002	0.1441	3.0069	12.3995	<0.003	<0.003	<0.002	84.5	<0.002	<0.00007	100.05	
MVT-32	El Zapote Spring	03/03/1997	30.2	<0.0002	0.027	0.2077	1.3515	0.01805	<0.0003	<0.0002	98.4	<0.0006	<0.00002	100.00	−7.0*

[a] Detection limits vary depending on the date of analysis and standardization. Carbon isotope values with asterisk are average of two analyses.

Table 8
Noble gas analyses and gas ratios on samples from the Jungapeo area, Mexico

Sample	Location	$^3He/^4He$ (R/Ra)	He/Ne $(He/Ne)_{Air}$	$^3He/^4He$ (Rc/Ra)	^4He (ppm)	Total Ne (ppm)	N_2 (%)	O_2 (%)	^{40}Ar (%)	^{36}Ar (ppm)	Total Kr (ppm)	$^{20}Ne/^{36}Ar$	$^{40}Ar/^{36}Ar$	N_2/Ar	He/Ne
MVT-23	El Tular	2.941	22.7	3.031	61.00	9.34	92.41	5.59	1.94	65.312	3.153	0.130	296	47.73	6.53
MVT-24	Cañada Azul	2.044	2.8	2.621	3.23	4.00	80.78	17.77	1.38	47.017	2.772	0.077	294	58.40	0.81
MVT-25	Agua Blanca	2.853	18.3	2.960	47.15	8.95	93.78	3.71	2.37	79.817	7.367	0.102	297	39.62	5.27
MVT-32	El Zapote	2.828	16.6	2.945	46.09	9.64	86.72	11.30	1.91	65.151	4.396	0.135	294	45.29	4.78

about 250 km east of Jungapeo. The plus symbols show another group of meteoric waters collected from the Popocatépetl region (Werner et al., 1997; F. Goff, unpublished data) that are matched by the range presented in Inguaggiato et al. (2005). Los Azufres meteoric waters and Jungapeo waters of all types are isotopically similar because of geographic proximity and roughly equivalent elevations, whereas Jungapeo waters are isotopically less depleted than most Mexico City Basin waters and Popocatépetl waters because the latter fluids issue farther from ocean sources of rain and at higher elevations.

The shaded circle on Fig. 16 shows the pre-production isotopic composition of the ca. 300 °C Los Azufres geothermal reservoir (Barragán et al., 2005). Los Azufres geothermal fluids are isotopically enriched by about 6‰ $\partial^{18}O$ relative to Los Azufres meteoric waters, a magnitude of enrichment commonly seen in high-temperature geothermal systems (Goff and Janik, 2000). Because Jungapeo waters show little, if any, enrichment in oxygen-18 relative to the WMWL, there is no evidence of high-temperature rock–water isotopic exchange in the Jungapeo system.

Several of the water samples are slightly depleted in oxygen-18 relative to the WMWL and the MBWL. Although this apparent depletion may be mostly analytical error, it may be that minor oxygen isotope exchange is occurring between CO_2 and H_2O in the tepid CO_2-rich waters. Such an exchange is promoted by cool temperatures and high CO_2 gas flux, and has been documented in waters at other CO_2-rich sites (Fritz and Frape, 1982; Vuataz and Goff, 1986; Matthews et al., 1987; Pauwels et al., 1997).

6.3. Relative ages of waters

The cold background sample from El Concreto has 2.1 TU tritium (^3H), a relatively typical value for recent rain in southern Mexico and Central America (Janik et al., 1992). However, Jungapeo thermal waters have lower ^3H ($\leq$1.8 TU, Table 4). The plot of tritium vs. chloride (Fig. 17) shows that most thermal waters plot as a group with no apparent trend. Thus, the aquifer feeding most of the springs has multiple recharge paths with different residence times inside the Tuxpan shield. El Aguacate, along the Río Tuxpan, stands out on Fig. 17 because of its much higher chloride content, but the relatively high ^3H of this sample implies dilution with river water (Fig. 11D). The ages of the Jungapeo mineral waters can be estimated using tables and methods described in Goff et al. (1991) and Shevenell and Goff (1995), respectively for piston-flow and well-mixed aquifers. Most Jungapeo thermal waters have high flow rates and are probably best modeled as piston-flow aquifers. Because they have 0.3 to 1.8 TU ^3H, their waters have calculated mean residence times (water ages) of about 7 to 25 years.

7. Gas geochemistry

Bulk chemistry of several Jungapeo area gas samples (Table 7) show the gases are extremely rich in CO_2 and are usually contaminated with air components (N_2, O_2, and Ar). From a geothermal perspective, the gases have no detectable H_2S or H_2 and very low contents of CH_4 and NH_3. Gas from El Aguacate spring is not distinguishable from gases at other Jungapeo sites. Carbon-13 isotope analyses of the CO_2 from many sites (Table 4) show a narrow range of values between −6.7‰ and −7.2‰. Although the carbon isotopes of Jungapeo CO_2 resemble the value for CO_2 in air (about −7‰), the concentration of CO_2 in air (0.04 mol%) is insignificant compared to the amount of CO_2 in Jungapeo gases ($\geq$90 mol%). Thus air is not a viable source for most of the CO_2. The isotopic composition of Jungapeo CO_2 indicates that most CO_2 could logically originate from the mantle, assuming a MORB value of −5‰ to −8‰ $\partial^{13}C$–CO_2 (Hoefs, 1973; Rollinson, 1993). Because

temperatures of 150 °C exist at relatively shallow depths beneath the TMVB, some CO_2 could be contributed to Jungapeo gases from thermal degradation of organic material in underlying Cretaceous marls and shales, a process that appears to produce most of the isotopically depleted CO_2 in The Geysers, California (Bergfeld et al., 2001). Thermal decarbonation of Cretaceous limestone at moderate temperatures can not be a major source of CO_2 in Jungapeo gases because the source carbonate would have to be more enriched in $\partial^{13}C$ than the produced CO_2 and most marine limestones have values between 0±4‰ $\partial^{13}C$ (Hoefs, 1973; Goff et al., 1985).

Noble gas data for four samples are listed in Table 8. The noble gases were analyzed from splits of headspace gas taken from the bulk gas samples. Unfortunately, a good noble gas split was not obtained from the El Aguacate site. One of the noble gas samples (Cañada Azul) is substantially contaminated with air. The other three samples contain less air contamination and are considered more representative of Jungapeo noble gases. The helium contents of the gases are low (≤61 ppm) but the $^{3/4}$He ratios corrected for air contamination range from about 2 to 3 Rc/Ra. These results indicate that a small mantle/magmatic component of helium-3 is present in Jungapeo gases.

The relative concentration of helium in Jungapeo gases can be examined in the N_2–Ar–He ternary of Fig. 18. Jungapeo gases have no helium excess and plot on the join between air saturated water and air. In contrast, gases from high-temperature geothermal systems (i.e., The Geysers, Yellowstone, and Valles caldera) or hot spot volcanoes (i.e. Kilauea and Sierra Negra) generally have relatively high bulk helium.

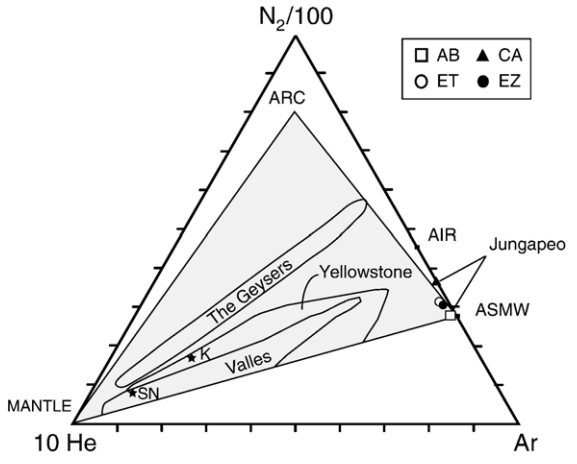

Fig. 18. Triangular plot of N_2/100-Ar-10He for gases of the Jungapeo area, Mexico, compared with gases from selected hot spots and high-temperature geothermal systems (modified from Giggenbach, 1992). Data sources: K (average Kilauea volcano, Hawaii) and SN (average Sierra Negra volcano, Galapagos) from Goff et al. (2000); Valles caldera and Yellowstone from Goff and Janik (2002); The Geysers from Lowenstern et al. (1999).

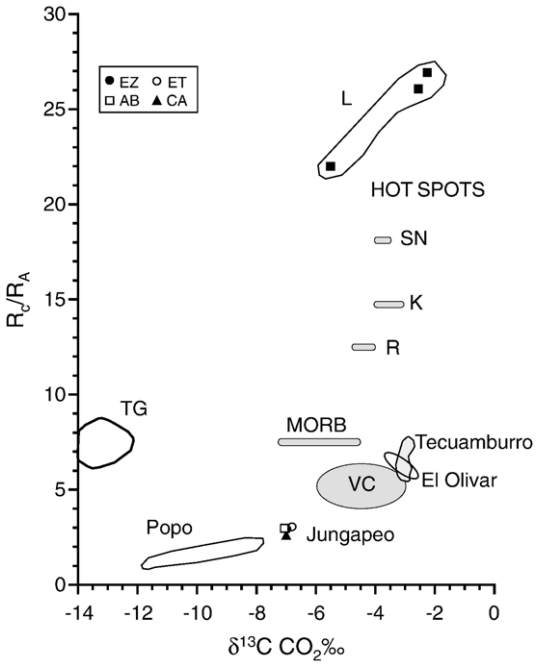

Fig. 19. Plot of $He^{3/4}$ versus $\partial^{13}C$–CO_2 for gases of the Jungapeo area, Mexico, compared with gases from hot spots, MORB and various geothermal systems. L=Loihi volcano, Hawaii (Sedwick et al., 1994); SN=Sierra Negra and K=Kilauea (both from Goff et al., 2000); R=Reunion (Marty et al., 1993); MORB=mid-ocean ridge basalt (Rollinson, 1993); VC=Valles caldera (Goff and Janik, 2002); TG=The Geysers (Bergfeld et al., 2001); Popo=Popocatépetl (Inguaggiato et al., 2005); Tecuamburro from Janik et al. (1992); El Olivar from Goff et al. (1987) and Kennedy et al. (1991).

A comparison of $He^{3/4}$ ratios and $\partial^{13}C$–CO_2 values between Jungapeo gases and other geothermal system and hot spot gases is shown in Fig. 19. Hot spot gases have $He^{3/4}$ ratios varying from 13 to 28 Rc/Ra, whereas MORB and high-temperature geothermal gases have ratios between 6 and 9 Rc/Ra. By comparison, Jungapeo $He^{3/4}$ ratios are small, only 2 to 3 Rc/Ra, about the same or slightly higher than those from Popocatépetl volcano area. Carbon-13 in CO_2 measured in hot spot gases range narrowly between −2‰ and −6‰ whereas MORB values range between −5‰ and −8‰. Geothermal gases have values ranging from −2 to less than −14‰ $\partial^{13}C$–CO_2. Geothermal gases with very depleted $\partial^{13}C$–CO_2 such as The Geysers contain substantial amounts of organic CO_2 from marine sedimentary rocks (Bergfeld et al., 2001) as mentioned above, whereas gases from geothermal systems underlain by marine limestone (e.g., Valles caldera,

Tecuamburro, and El Olivar) often contain a mixture of mantle and marine limestone sources (Janik et al., 1992; Goff and Janik, 2002). Because Jungapeo is underlain in part by Cretaceous marls and shales, some CO_2 gas could be derived from organic sources, although most CO_2 seems to originate from a MORB-like source.

8. Chemical geothermometry

Thermal equilibration of the Jungapeo waters can be evaluated in the Na–K–Mg ternary (Fig. 20) devised by Giggenbach (1988). Most Jungapeo waters plot near the $Mg^{1/2}$ apex and are considered to be cold and "immature". In contrast, EA waters form a linear cluster straddling the 175 °C temperature line for full equilibration. The position of the cluster suggests that EA waters are now partly equilibrated or mixed fluids, in which cooler Mg-rich waters dilute a relatively high-temperature fluid component.

Calculated subsurface reservoir temperatures of various Jungapeo fluids can be compared in Table 9 using a standard suite of chemical geothermometers (Urbani, 1986). The calculations vary tremendously because Jungapeo waters show multiple processes such as equilibration at high and low temperatures, mixing of fluids and re-equilibration of mixed fluids. Interpretation of chemical geothermometers is complicated in low- to moderate-temperature situations because many of the geothermometers are empirically derived from the chemistry of high-temperature fluids (Fournier, 1981; Goff and Janik, 2000). In spite of these difficulties, our preferred temperature estimates are shown in bold on Table 9. We have divided the waters into four groups: A deep water represented by El Aguacate, two types of very similar shallow waters exemplified by Agua Blanca and Cañada Azul, respectively, and background water represented by El Concreto.

El Aguacate spring produces the only water that indicates derivation from a moderate- to high-temperature geothermal aquifer. The best estimated temperature for this source fluid is around 150 to 175 °C (Fig. 20 and Table 9). The spring discharges along the Río Tuxpan; thus it is undoubtedly mixed with some river water. Discharge temperature–chloride relations also indicate mixing, as do many of the other plots described above. Because the quartz conductive geothermometer indicates a substantially lower temperature (128 °C) than 150 to 175 °C, mixing of high- and low-temperature components is indicated. Temperature re-equilibration is implied by the Mg–Li and K–Mg geothermometers, which indicate subsurface temperature of only 80 to 100 °C (Giggenbach, 1988; Kharaka and Mariner, 1989).

Jungapeo shallow mineral waters are derived from a large aquifer system that circulates in the young Tuxpan shield volcano E of the Río Tuxpan. Temperatures calculated from the amorphous silica and Na–K–Ca (Mg-corrected) geothermometers are nearly identical to

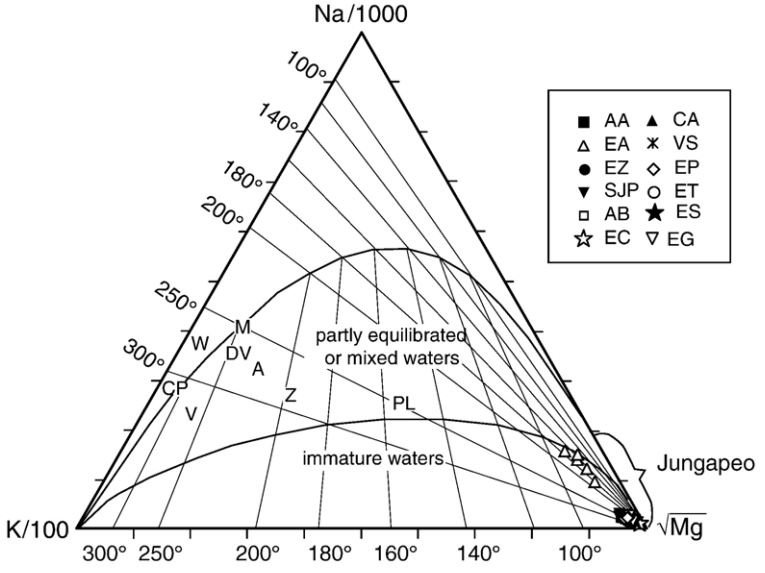

Fig. 20. Triangular plot of Na/1000-K100-$Mg^{1/2}$ for waters of the Jungapeo area, Mexico, compared with waters from high-temperature geothermal systems and from the low-temperature waters at Popocatépetl (Werner et al., 1997, Table 10 and Goff and Janik, 2000, Table 3). Labels: A = Ahauchapán; W = Wairakei, CP = Cerro Prieto; DV = Dixie Valley; PL = Platanares; V = Valles caldera; M = Miravalles; Z = Zunil; AH = Agua Hedionda; OX = Oaxtepec; IX = Ixtatlala.

Table 9
Estimated reservoir temperature of Jungapeo thermal waters using a standard suite of chemical geothermometers (Urbani, 1986). All values are in °C except where noted. Our preferred temperature estimate for each water type is shown in bold characters. Temperatures in parentheses violate the application rules of the geothermometer in question but are shown to complete the table

Site	N[a]	Measured temperature	$T_{(Amorph)}$[b]	$T_{(Chal)}$[b]	$T_{(Qtz\ cond)}$[b]	$T_{(Na/K)t}$[c]	$T_{(Na/Li)d}$[d]	$T_{(Na–K–Ca)}$ (B=1/3)[e]	$T_{(Na–K–Ca)}$ (B=4/3)[e]	$T_{(Na–K–Ca–Mg)}$[f]	R[f]	$T_{(Mg/Li)}$[g]	$T_{(K/Mg)}$[h]	$T_{(D–P)}$[i]
"Deep" water														
El Aguacate	5	33.4±1.2 (4)	9±7	100±9	128±8	104±11	132 (1)	**150±8**	{147±19}	37±13	38±7	98 (1)	83±5	49 (1)
"Shallow" water, Group I														
San José Purúa	12	32.0±0.3 (7)	**32±9**	129±11	154±10	191±22	198±2 (2)	{172±9}	100±7	**32±6 (3)**	51±3	72±1 (2)	64±4	47±3 (2)
Agua Blanca	14	29.9±0.5 (9)	**25±5**	120±6	146±5	195±22	195±4 (2)	{172±8}	95±5	**35±5 (5)**	50±3	68±1 (2)	62±2	41±1 (2)
El Puente	4	29.1±0.1	**24±6 (3)**	112±16	139±15	208±25	nd	{176±11}	96±7	**33 (1)**	51±3	nd	63±4	nd
Agua Amarilla	13	30.8±0.2 (8)	**26±8**	122±10	147±9	186±18	197 (1)	{169±9}	95±8	**34±4 (3)**	51±3	68 (1)	62±4	50 (1)
El Tular	12	29.4±0.5 (7)	**24±11**	119±14	145±13	196±19	195 (1)	{172±8}	93±6	**31±3 (7)**	50±3	66 (1)	62±3	40 (1)
"Shallow" water, Group II														
Cañada Azul	13	27.1±0.9 (8)	**20±9**	114±11	141±10	214±41	193 (1)	{175±13}	86±7	**37±4 (5)**	50±3	61 (1)	59±3	42 (1)
Varelas	3	29.8±0.3	**20±8**	115±9	141±9	185±5	174 (1)	{162±5}	77±10	**<50 (cool)**	43±16	53 (1)	57±3	nd
El Sauz	3	28.4±0.4	**20±4**	114±6	141±5	201±16	174 (1)	{168±8}	79±8	**<50 (cool)**	56±1	48 (1)	53±5	nd
El Gauyabo	2	29.7±0.3	**16±13**	109±16	136±15	173±26	179 (1)	{160±7}	85±4	**<50 (cool)**	56±1	52 (1)	54±1	50 (1)
El Zapote	3	29.7±0.6	**21±9**	116±11	142±10	198±1	180 (1)	{170±2}	85±3	**<50 (cool)**	58±2	53 (1)	55±1	38 (1)
Background water														
El Concreto	1	24.5	**19**	113	140	229	165	{175}	74	**<50 (cool)**	64	36	47	nd

[a] Number of analyses available for the averaged calculations; numbers in parentheses show the value of n in cases where parameters are lacking.
[b] Amorphous silica, chalcedony, and quartz conductive equations in Fournier (1981).
[c] Na–K equation of Truesdell as reported in Fournier (1981).
[d] Na–Li equation for dilute waters of Fouillac and Michard (1981).
[e] Na–K–Ca equations of Fournier and Truesdell (1973).
[f] Na–K–Ca–Mg equation and calculated R-value of Fournier and Potter (1979).
[g] Mg–Li equation of Kharaka and Mariner (1989).
[h] K–Mg equation of Giggenbach et al. (1983) and Giggenbach (1988).
[i] CO_2–H_2S–H_2–CH_4 equation of D'Amore and Panichi (1980). Average equilibrium temperature (if values are below detection limits, we used 0.001 H_2, 0.0001 CH_4, and 0.001 H_2S in geothermometer calculations).

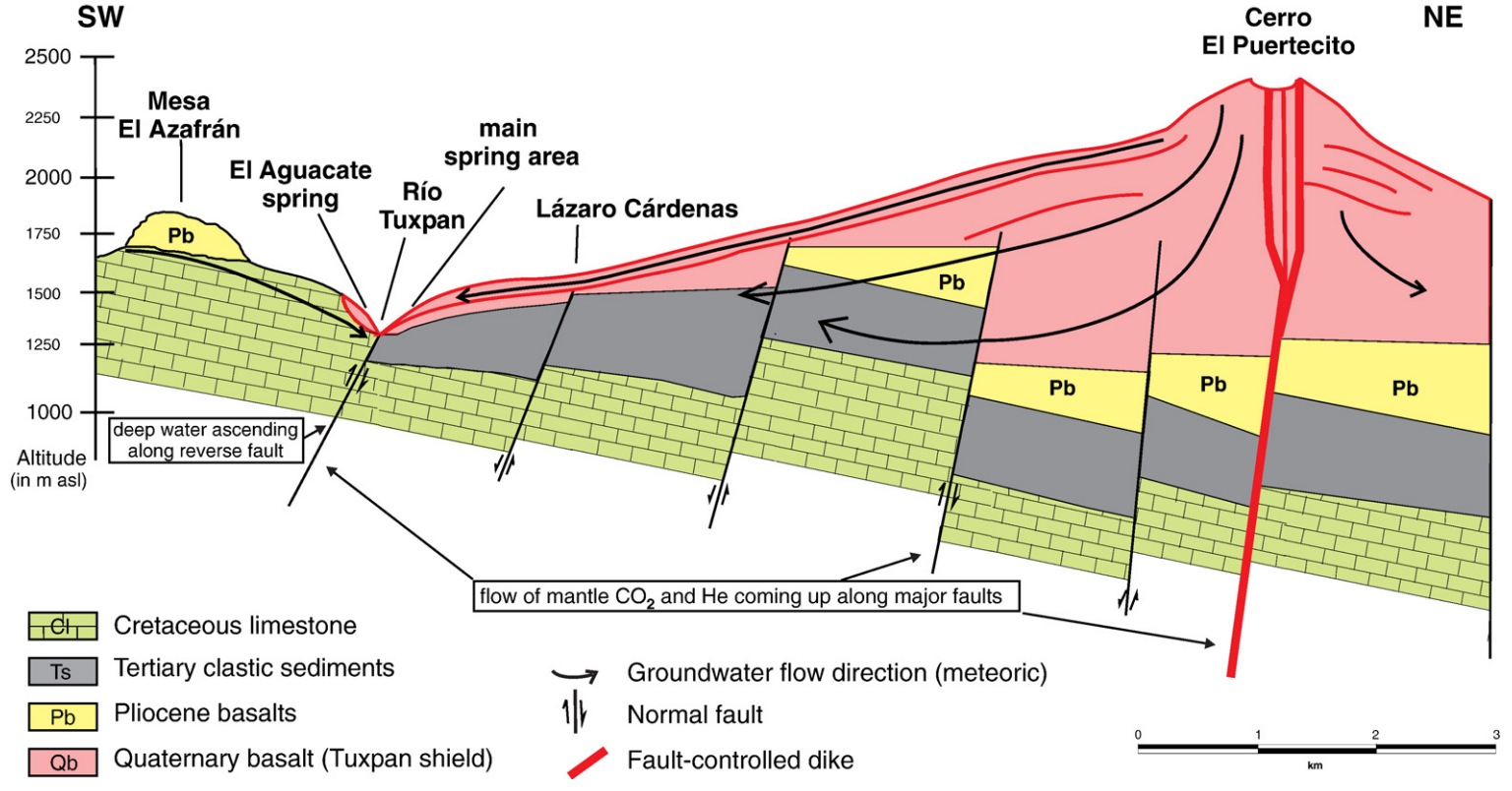

Fig. 21. NE–SW cross-section through the Jungapeo area, Mexico showing our conceptual model of the geothermal system. Profile shown is located on Fig. 2.

discharge temperatures (roughly 30 °C). Although some trace elements show relatively high values (i.e., B), As contents are extremely low and other constituents such as Ca, Mg, and Fe are much higher than those found in typical high-temperature geothermal fluids (Goff and Janik, 2000). Paces (1975) noted that the Na–K–Ca geothermometer was not reliable for CO_2-rich waters equilibrated below 75 °C and other geothermal investigators have noted that Mg-rich waters cannot equilibrate at temperatures above 75 °C (i.e., Fournier and Potter, 1979). Based on such considerations, it is our opinion that high CO_2 and resulting HCO_3 aggressively attack the basaltic andesite (especially olivine and clinopyroxene crystals) in the Tuxpan shield volcano, dissolving copious amounts of SiO_2, Fe, Ca, Mg, and some trace elements to produce mineralized waters superficially resembling higher temperature geothermal fluids. Thus, most geothermometers predict excessively high temperatures for the shallow Jungapeo waters.

Gas geothermometers indicate relatively cool temperatures of subsurface equilibration (≤ 50 °C). There are no apparent differences between the gases derived from EA and other Jungapeo sites.

The background water, El Concreto, contains some shallow mineralized water as described above. We were not able to find a completely uncontaminated sample of cold background water in the immediate vicinity of the Tuxpan shield volcano.

9. Geothermal system model

The main features of our conceptual model of the geothermal system feeding the mineral springs are shown in Fig. 21. In this model, NNW–SSE oriented older reverse faults (Pasquaré et al., 1988) are superimposed by a set of younger parallel extensional normal faults that produce a step-faulted pattern. These faults have served as conduits for ascending batches of magma that upon eruption constructed the diverse volcanoes occurring in the area. These include the NNW–SSE oriented cones from which the voluminous lavas of the Tuxpan shield emanated. Accordingly, segments of larger faults are occupied by cooling and degassing dikes that must reach deep into the crust and mantle and serve as pathways for gases (e.g. He and some CO_2) of mantle origin. Meteoric water precipitating on the surface of the Tuxpan shield easily percolates downward until reaching impermeable layers (marls and shales) of the local Cretaceous basement. This water is heated by remnant heat from the magma bodies in the TMVB and possibly by small shallow magma bodies of the basaltic shield. Some CO_2 may originate by thermal degradation of organic remains in underlying marine rocks. Assuming a reasonable conductive thermal gradient of 60 °C/km for this region (Prol-Ledsema and Juárez, 1986; Prol-Ledesma, 1991) and an ambient temperature of 18 °C (Fig. 10), the depth to a 175 °C aquifer as indicated by the geothermometers is roughly 2.5 km. We hesitate to call this deep aquifer a geothermal "reservoir" because only one of the Jungapeo sites (El Aguacate) discharges water with high-temperature characteristics.

Meteoric waters mix with rising, gas-rich thermal fluids to form slightly acidic, bicarbonated waters that react with host rocks releasing soluble constituents. Horizontal flow and permeability discordances along faults force these waters to return into the permeable Tuxpan shield lava flows at more distal and lower elevations, where they corrode olivine and pyroxene crystals (iddingsitization) and hydrate and leach the matrix glass. The CO_2-saturated groundwater finally emerges deep in the Tuxpan River canyon at the contact of the lavas with the underlying less permeable marine basement. When cooling down to ambient temperatures in pools and streamlets, opaline silica, calcite, goethite, etc., precipitate and form travertine coatings.

10. Concluding remarks

The CO_2-rich mineral waters of the Jungapeo area hint at first sight toward the existence of a high-enthalpy geothermal system. This idea is favored by the nearby occurrence of the Los Azufres geothermal field. The youngest (<0.60 Ma) volcanic edifices are monogenetic scoria cones, domes, and related lava flows whose compositions point toward a deep magmatic source in the lithospheric mantle. Although closely linked in space and time, whole-rock chemical analyses of the scoria cones and lavas exclude the existence of a common large magma chamber at shallow crustal levels that would be capable of inducing a high-enthalpy geothermal system.

In consequence, the Jungapeo geothermal system is not capable of electricity production. Furthermore, the bicarbonated waters might be difficult to use in space heating and other industrial applications due to the risk of CO_2 release and precipitation of carbonates. However, the spring waters are ideal for balneological purposes. The benign properties of the waters to humans are underscored by the fact that our analyses did not detect any toxic elements (e.g. high arsenic contents) or an elevated level of radioactivity. In this sense we hope that the municipal authorities of Jungapeo preserve the natural beauty of this area for the enjoyment of future generations.

Acknowledgments

C. Siebe was funded by grants CONACYT-50677-F and DGAPA-UNAM-IN-101006-3. F. Goff, D. Counce, R. Poreda, and S. Chipera were funded by an Institutional Supporting Research and Development grant (Magmatic Tritium) to F. Goff from Los Alamos National Laboratory (1995–1997). A. Aguayo, N. Cenizeros, and O. Cruz (UNAM) carried out chemical analyses of part of the water samples. Michael Abrams (Jet Propulsion Laboratory) provided Landsat satellite imagery funded by NASA. Climate data obtained at Laguna El Freso meteorological station was kindly provided by Ing. Javier Espinosa Cruickshank (Servicio Meteorológico Nacional). Figures were drafted by Deborah Bergfeld (US Geological Survey) and by Ignacio Hernández Javier, Lilia Arana Salinas, and Renato Castro Govea (UNAM). Petrographic work was carried out with the aid of a new Leitz polarizing microscope donated by the Alexander von Humboldt Foundation (Germany) to C. Siebe. Dawnika Blatter and Alain Demant freely shared information obtained during their earlier work in the study area. The manuscript was kindly reviewed by S. Inguaggiato (Palermo, Italy), G. Chiodini (Naples, Italy), and an anonymous reviewer.

References

Armienta, M.A., De la Cruz-Reyna, S., 1995. Some hydrogeochemical fluctuations observed in Mexico related to volcanic activity. Applied Geochemistry 10, 215–227.

Baker, I., Haggerty, E.S., 1967. The alteration of olivine in basaltic and associated lavas: Part II. Intermediate and low temperature alteration. Contributions to Mineralogy and Petrology 16, 258–273.

Barnes, I., O'Neil, J.R., Rapp, J.B., White, D.E., 1973. Silica–carbonate alteration of serpentine: wall rock alteration in mercury deposits of the California Coast Ranges. Economic Geology 68, 388–398.

Barragán, R.M., Arellano, V.M., Portugal, E., Sandoval, F., 2005. Isotopic (∂^{18}O, D) patterns in Los Azufres (Mexico) geothermal fluids related to reservoir exploitation. Geothermics 34, 527–547.

Bergfeld, D., Goff, F., Janik, C.J., 2001. Carbon isotopes and CO_2 sources in The Geysers–Clear Lake region, northern California. Geothermics 30, 303–331.

Blatter, D.L., Carmichael, I.S.E., 1998. Plagioclase-free andesites from Zitácuaro (Michoacán), Mexico; petrology and experimental constraints. Contributions to Mineralogy and Petrology 132, 121–138.

Blatter, D.L., Carmichael, I.S.E., Deino, A.L., Renne, P.R., 2001. Neogene volcanism at the front of the central Mexican volcanic belt: basaltic andesites to dacites, with contemporaneous shoshonites and high-TiO_2 lava. Geological Society of America Bulletin 113, 1324–1342.

Capra, L., Macías, J.L., Garduño, V.H., 1997. The Zitácuaro Volcanic Complex, Michoacán, Mexico: magmatic and eruptive history of a resurgent caldera. Geofísica Internacional 36, 161–179.

Chipera, S.J., Bish, D.L., 2002. FULLPAT: a full-pattern quantitative analysis program for X-ray powder diffraction using measured and calculated patterns. Journal of Applied Crystallography 35, 744–749.

Choi, H.-S., Koh, Y.-K., Bae, D.-S., Park, S.-S., Hutcheon, I., Yun, S.-T., 2005. Estimation of deep-reservoir temperature of CO_2-rich springs in Kangwon district, South Korea. Journal of Volcanology and Geothermal Research 77, 77–89.

Cortés, A., Durazo, J., Farvolden, R.N., 1997. Studies of isotopic hydrology of the Basin of Mexico and vicinity: annotated bibliography and interpretation. Journal of Hydrology 198, 346–376.

Craig, H., 1961. Isotopic variations in meteoric waters. Science 133, 1702–1703.

D'Amore, F., Panichi, C., 1980. Evaluation of deep temperatures of hydrothermal systems by a new gas geothermometer. Geochimica Cosmochimica Acta 44, 549–556.

Demant, A., Mavois, R., Silva Mora, L., 1975. Estudio geológico de las hojas Morelia y Maravatío, Estado de Michoacán. Comisión Federal de Electricidad, Instituto de Geología, Universidad Nacional Autónoma de México. 53 pp.

Dobson, P.F., Mahood, G.A., 1985. Volcanic stratigraphy of the Los Azufres geothermal area, Mexico. Journal of Volcanology and Geothermal Research 25, 273–287.

Fahlquist, L., Janik, C.J., 1992. Procedures for collecting and analyzing gas samples from geothermal systems. U.S. Geological Survey, Open-file Report 92-211. 19 pp.

Fouillac, C., Michard, G., 1981. Sodium/lithium ratio in water applied to geothermometry of geothermal reservoirs. Geothermics 10, 55–70.

Fournier, R.O., 1981. Application of water chemistry to geothermal exploration and reservoir engineering. In: Rybach, L., Muffler, L.J.P. (Eds.), Geothermal Systems: Principles and Case Histories. Wiley, New York, pp. 109–143.

Fournier, R.O., Potter, R.W., 1979. Magnesium correction to the Na–K–Ca chemical geothermometer. Geochimica Cosmochimica Acta 43–9, 1543–1550.

Fournier, R.O., Truesdell, A.H., 1973. An empirical Na–K–Ca geothermometer for natural waters. Geochimica Cosmochimica Acta 37, 1255–1275.

Fritz, P., Frape, S.K., 1982. Comments on the ^{18}O, ^{2}H and chemical composition of saline groundwaters in the Canadian Shield. In: Perry, E.C. (Ed.), Isotopic Studies of Hydrologic Processes. Northern Illinois University Press, De Kalb, Illinois, pp. 57–63.

Giggenbach, W.F., 1988. Geothermal solute equilibria: Derivation of Na–K–Ca–Mg geoindicators. Geochimica Cosmochimica Acta 52, 2749–2765.

Giggenbach, W.F., 1992. Chemical techniques in geothermal exploration. In: D'Amore, F. (Ed.), Applications of Geochemistry in Geothermal Reservoir Development. Series of Technical Guides on the Use of Geothermal Energy, UNITAR/UNDP Centre on Small Energy Resources, Rome, Italy, pp. 119–144.

Giggenbach, W.F., Gonfiantini, R., Jangi, B.L., Truesdell, A.H., 1983. Isotopic and chemical composition of Parbati Valley geothermal discharges, N.W. Himalayas, India. Geothermics 12, 199–222.

Goff, F., unpublished. Geochemical data from Mexico volcanic and geothermal areas collected 1994 to 2002, Author files.

Goff, F., Janik, C.J., 2000. Geothermal systems. In: Sigurdsson, H., Houghton, B., McNutt, S., Rymer, H., Stix, J. (Eds.), Encyclopedia of Volcanoes. Academic Press, San Diego, CA, pp. 817–834.

Goff, F., Janik, C.J., 2002. Gas geochemistry of the Valles caldera region, New Mexico, and comparisons with gases at Yellowstone,

Long Valley and other geothermal systems. Journal of Volcanology and Geothermal Research 116, 299–323.
Goff, F., McMurtry, G.M., 2000. Tritium and stable isotopes of magmatic waters. Journal of Volcanology and Geothermal Research 97, 347–396.
Goff, F., Gardner, J., Vidale, R., Charles, R., 1985. Geochemistry and isotopes of fluids from Sulphur Springs, Valles Caldera, New Mexico. Journal of Volcanology and Geothermal Research 23, 273–297.
Goff, F., Truesdell, A.H., Grigsby, C.O., Janik, C.J., Shevenell, L., Paredes, R., Gutierrez, J.W., Trujillo, P.E., Counce, D., 1987. Hydrogeochemical investigation of six geothermal sites, Honduras, Central America. Los Alamos National Laboratory, Report LA-10785-MS. 200 pp. (obtainable from the second author).
Goff, F., Goff, S.J., Kelkar, S., Shevenell, L., Truesdell, A., Musgrave, J., Rufenacht, H., Flores, W., 1991. Exploration drilling, reservoir testing, age, and reservoir model of the Platanares geothermal system, Honduras, Central America. Journal of Volcanology and Geothermal Research 45, 101–124.
Goff, F., McMurtry, G.M., Counce, D., Stimac, J.A., Roldán-Manzo, A., Hilton, D., 2000. Contrasting hydrothermal activity at Sierra Negra and Alcedo volcanoes, Galapagos Archipelago, Ecuador. Bulletin of Volcanology 62, 34–52.
Hasenaka, T., Carmichael, I.S.E., 1985. The cinder cones of Michoacán–Guanajuato, central Mexico: their age, volume and distribution, and magma discharge rate. Journal of Volcanology and Geothermal Research 25, 105–124.
Hasenaka, T., Carmichael, I.S.E., 1987. The cinder cones of Michoacán–Guanajuato, central Mexico; petrology and chemistry. Journal of Petrology 28, 241–269.
Hoefs, J., 1973. Stable Isotope Geochemistry. Springer, New York. 140 pp.
Inguaggiato, S., Martin-Del Pozzo, A.L., Aguayo, A., Capasso, G., Favara, R., 2005. Isotopic, chemical, and dissolved gas constraints on spring water from Popocatépetl volcano (Mexico): evidence of gas–water interaction between magmatic component and shallow fluids. Journal of Volcanology and Geothermal Research 141, 91–108.
Janik, C.J., Goff, F., Fahlquist, L., Adams, A., Roldán, A., Trujillo, P.E., Counce, D., 1992. Hydrogeochemical exploration of geothermal prospects in the Tecuamburro volcano region, Guatemala. Geothermics 21, 447–481.
Kennedy, B.M., Hiyagon, H., Reynolds, J.H., 1991. Noble gases from Honduras geothermal sites. Journal of Volcanology and Geothermal Research 45, 29–39.
Kharaka, Y.K., Mariner, R.H., 1989. Chemical geothermometers and their application to formation waters from sedimentary basins. In: Naeser, N.D., McCulloh, T.H. (Eds.), Thermal History of Sedimentary Basins, Methods and Case Histories. Springer, New York, pp. 99–177.
Krauskopf, K.B., 1979. Introduction to Geochemistry. McGraw-Hill, New York. 617 pp.
Les Bas, M.J., Le Maitre, R.W., Streckeisen, A., Zanettin, B., 1986. A chemical classification of volcanic rocks based on the total alkali–silica diagram. Journal of Petrology 27, 745–750.
Lowenstern, L.B., Janik, C.J., Fahlquist, L.S., Johnson, L.S., 1999. Gas and isotope geochemistry of 81 steam samples from wells in The Geysers geothermal field, Sonoma and Lake Counties, California, USA. U.S. Geological Survey, Open-file Report 99-304. 28 pp.
Luhr, J.F., Simkin, T., 1993. Paricutín – The Volcano Born in a Mexican Cornfield. Geoscience Press, Inc., Phoenix, Arizona. 427 pp.
MacDonald, G.A., Katsura, T., 1964. Chemical composition of Hawaiian lavas. Journal of Petrology 5, 82–133.
Marques, J.M., Matias, M.J., Basto, M.J., Graça, R.C., Aires-Barros, L., Andrade, M., Carreira, P.M., Goff, F., Rocha, L., 2004. Water–rock interaction responsible for the origin of high pH mineral waters (S-Portugal). Transactions Water–Rock Interaction 11, Wanty & Seal (eds), p. 293–297.
Marty, B., Meynier, V., Nicolini, E., Griesshaber, E., Toutain, J.P., 1993. Geochemistry of gas emanations: a case study of the Réunion Hot Spot, Indian Ocean. Applied Geochemistry 8, 141–152.
Matthews, A., Fouillac, C., Hill, R., O'Nions, R.K., Oxburgh, E.R., 1987. Mantle-derived volatiles in continental crust: the Massif Central of France. Earth and Planetary Science Letters 85, 177–128.
McLeod, R.G., 1989. Geology and tectonics of El Bosque area, Michoacán, Mexico. Master's thesis, Brigham Young University, Provo, Utah, 39 p.
Ostlund, H.G., Dorsey, H.G., 1977. Rapid electrolytic enrichment and hydrogen gas proportional counting of tritium, in Low Radioactivity Measurements. Proceedings of the International Conference on Low Radioactivity Measurements and Applications, 6–10 October 1975, The High Tatras, Czechoslovakia, Slovenske Pedagogicke, Nakladantelístvo, Bratislava. 5 pp.
Paces, T., 1975. A systematic deviation from Na-K-Ca geothermometer below 75 °C and 10^{-4} atm P_{CO2}. Geochimica Cosmochimica Acta 39, 541–545.
Pasquaré, G., Garduño, V.H., Tibaldi, A., Ferrari, L., 1988. Stress pattern evolution in the central sector of the Mexican Volcanic Belt. Tectonophysics 146, 353–364.
Pasquaré, G., Ferrari, L., Garduño, V.H., Tibaldi, A., Vezzoli, L., 1991. Geologic map of the central sector of the Mexican Volcanic Belt, States of Guanajuato and Michoacán, Mexico. Geological Society of America Map and Chart Series MCH072, pp. 1–19.
Pauwels, H., Fouillac, C., Goff, F., Vuataz, F.-D., 1997. The isotopic and chemical composition of CO_2-rich thermal waters in the Mont Dore region (Massif-Central, France). Applied Geochemistry 12, 411–427.
Petersen, M.D., 1989. Geology and tectonics of the Jungapeo, Michoacán, Mexico area and its relationship to the Mexican Volcanic Belt. Master's thesis, Brigham Young University, Provo, Utah, 26 p.
Poreda, R., Craig, H., 1989. Helium isotope ratios in circum-Pacific volcanic arcs. Nature 338, 473–478.
Pradal, E., Robin, C., 1994. Long-lived magmatic phases at Los Azufres volcanic center, Mexico. Journal of Volcanology and Geothermal Research 63, 201–215.
Prol-Ledesma, R.M., 1991. Terrestrial heat flow in Mexico. In: Cermak, V., Rybach, L. (Eds.), Exploration of the Deep Continental Crust. Terrestrial Heat Flow and the Lithosphere Structure. Springer-Verlag, Berlin, pp. 475–485.
Prol-Ledsema, R.M., Juárez, G., 1986. Geothermal map of Mexico. Journal of Volcanology and Geothermal Research 28, 351–362.
Rollinson, H., 1993. Using Geochemical Data: Evaluation, Presentation, Interpretation. Wiley, New York. 325 pp.
Schaaf, P., Stimac, J., Siebe, C., Macías, J.L., 2005. Geochemical evidence for mantle origin and crustal processes in products from Popocatépetl and surrounding monogenetic volcanoes, Central Mexico. Journal of Petrology 46, 1243–1282.
Sedwick, P.N., McMurtry, G.M., Hilton, D.R., Goff, F., 1994. Carbon dioxide and helium in hydrothermal fluids from Loihi Seamount, Hawaii: temporal variability and implications for the release of mantle volatiles. Geochimica Cosmochimica Acta 58, 1219–1227.

Shevenell, L., Goff, F., 1995. The use of tritium in groundwater to determine fluid mean residence times of Valles caldera hydrothermal fluids, New Mexico, USA. Journal of Volcanology and Geothermal Research 67, 187–205.

Siebe, C., Rodríguez-Lara, V., Schaaf, P., Abrams, M., 2004. Geochemistry, Sr–Nd isotope composition and tectonic setting of Holocene Pelado, Guespalapa, and Chichinautzin scoria cones, south of Mexico City. Journal of Volcanology and Geothermal Research 130, 197–226.

Sun, S.S., McDonough, W.F., 1989. Chemical and isotopic systematics of oceanic basalts: implications for mantle composition and processes. In: Saunders, A.D., Norry, M.J. (Eds.), Magmatism in the Ocean Basins. Geological Society Special Publication, vol. 42, pp. 313–345.

Torres-Alvarado, I., Satir, M., Fortier, S., Metz, P., 1995. An oxygen isotope study of hydrothermally altered rocks at the Los Azufres geothermal field, Mexico. Proceedings of the World Geothermal Congress, vol. 2. International Geothermal Association, Inc., Auckland, New Zealand, pp. 1049–1052.

Urbani, F., 1986. GTHERM, a spreadsheet and graphic setup for geothermal exploration. Unpub. Report, Los Alamos National Laboratory, NM, 103 pp.

Vuataz, F.-D., Goff, F., 1986. Isotope geochemistry of thermal and non-thermal waters in the Valles Caldera, Jemez Mountains, northern New Mexico. Journal of Geophysical Research 93, 6059–6067.

Werner, C., Janik, C., Goff, F., Counce, D., Johnson, L., Siebe, C., Delgado, H., Williams, S., Fischer, T., 1997. Geochemistry of summit fumarole vapors and flanking thermal/mineral waters at Popocatépetl Volcano, Mexico. Los Alamos National Laboratory, Report LA-13289-MS. 33 pp. (obtainable from the first or second authors).